5950 *Organometallics* **2007,** *26,* 5950−5960

Reactions of H_2 and R_3SiH with Electrophilic Cobalt(III) Alkyl Complexes: Spectroscopic Characterization, Dynamics, and Chemistry of $[Cp^*Co(L)(H)(\eta^2\text{-}H_2)][B(Ar_F)_4]$ and $[Cp^*Co(L)(H)(\eta^2\text{-}HSiR_3)][B(Ar_F)_4]$

Mark D. Doherty, Brian Grant, Peter S. White, and Maurice Brookhart*

Department of Chemistry, University of North Carolina at Chapel Hill, Chapel Hill, North Carolina 27599

Received June 21, 2007

Co(III) agostic alkyl complexes $[Cp^*Co(L)(CH_2CH_2\text{-}\mu\text{-}H)][B(Ar_F)_4]$ ($Cp^* = C_5(CH_3)_5$, L = $P(OCH_3)_3$, **1a**, or $P(CH_3)_3$, **1b**; Ar_F = 3,5-$(CF_3)_2C_6H_3$) react with H_2 to yield ethane and trihydride complexes characterized as η^2-dihydrogen hydride species $[Cp^*Co(L)(H)(\eta^2\text{-}H_2)][B(Ar_F)]$, **2a** and **2b**, in which there is rapid scrambling between the η^2-H_2 ligand and the terminal Co−H. Complexes **2a** and **2b** react with a variety of neutral donor ligands (L′ = RCN, PMe_3, $P(OMe)_3$, H_2O, CH_3OH) to yield $[Cp^*Co(L)(L')(H)][B(Ar_F)_4]$ complexes. Reaction of silanes with either **1a**,**b** in the presence of traces of water or **2a**,**b** yields η^2-silane hydrides, $[Cp^*Co(L)(H)(\eta^2\text{-}HSiR_3)][B(Ar_F)_4]$. Analysis of the dynamics of these species by NMR spectroscopy provides evidence for an extremely rapid process involving silyl migration between hydrogens and a slower process in which a cobalt-silyl η^2-H_2 complex is formed as an intermediate and results in hydrogen scrambling between the two diastereomers of $[Cp^*Co(L)(H)(\eta^2\text{-}H\text{-}SiHMePh)][B(Ar_F)_4]$. The structures and dynamics of **2a**,**b** and the η^2-silane complexes imply that cleavage of the cobalt−alkyl bonds of **1a**,**b** in hydrogenation and hydrosilation catalytic cycles occurs by the σ-CAM (σ-complex-assisted metathesis) process.

Introduction

Interest in the structure and chemistry of highly electrophilic late transition metal complexes has escalated over the past two decades due to their increasing application in catalytic transformations as well as the ability to stabilize and characterize highly reactive unsaturated cationic late metal complexes through the use of inert, weakly coordinating counteranions, particularly fluorinated aryl borate anions. Notable examples include Ir(III) complexes of the type $Cp^*Ir(PMe_3)R^+$, which are active for sp^3-C−H bond activations,[1,2] and Ni(II) and Pd(II) complexes of general structure $(L{-}L)MR^+$, many of which are active catalysts for olefin dimerizations,[3−5] oligomerizations,[6,7] and polymerizations,[8,9] olefin/CO copolymerizations,[10−13] and hydrosilation[14] reactions.

We have had an ongoing interest in the chemistry of electrophilic complexes of the general structure $(C_5R_5)(L)CoR^+$.[15−27] These formally 16-electron alkyl complexes, **1**, exhibit β-agostic interactions (R = ethyl or greater) and are highly dynamic.[15,19,21,25] Rotation around the C_α−C_β bond is rapid ($\Delta G^\ddagger$ = 11−12 kcal/mol), and the metal can migrate along the carbon chain through a series of β-H elimination/olefin rotation/reinsertion reactions, now commonly termed chain-walking processes.[15−17,19]

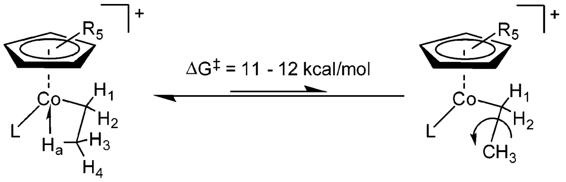

These species serve as living ethylene polymerization catalysts,[16,20,21,25−27] α-olefin oligomerization catalysts,[15] and

---

* Corresponding author. E-mail: mbrookhart@unc.edu.

(1) Golden, J. T.; Andersen, R. A.; Bergman, R. G. *J. Am. Chem. Soc.* **2001**, *123*, 5837−5838.

(2) Klei, S. R.; Tilley, T. D.; Bergman, R. G. *J. Am. Chem. Soc.* **2000**, *122*, 1816−1817.

(3) Ledford, J.; Shultz, C. S.; Gates, D. P.; White, P. S.; DeSimone, J. M.; Brookhart, M. *Organometallics* **2001**, *20*, 5266−5276.

(4) Rix, F. C.; Brookhart, M. *J. Am. Chem. Soc.* **1995**, *117*, 1137−1138.

(5) Shultz, C. S.; DeSimone, J. M.; Brookhart, M. *Organometallics* **2001**, *20*, 16−18.

(6) Svejda, S. A.; Brookhart, M. *Organometallics* **1999**, *18*, 65−74.

(7) Killian, C. M.; Johnson, L. K.; Brookhart, M. *Organometallics* **1997**, *16*, 2005−2007.

(8) Johnson, L. K.; Killian, C. M.; Brookhart, M. *J. Am. Chem. Soc.* **1995**, *117*, 6414−6415.

(9) Ittel, S. D.; Johnson, L. K.; Brookhart, M. *Chem. Rev.* **2000**, *100*, 1169−1203.

(10) Brookhart, M.; Wagner, M. I. *J. Am. Chem. Soc.* **1996**, *118*, 7219−7220.

(11) Rix, F. C.; Brookhart, M.; White, P. S. *J. Am. Chem. Soc.* **1996**, *118*, 4746−4764.

(12) Shultz, C. S.; Ledford, J.; DeSimone, J. M.; Brookhart, M. *J. Am. Chem. Soc.* **2000**, *122*, 6351−6356.

(13) Drent, E.; Budzelaar, P. H. M. *Chem. Rev.* **1996**, *96*, 663−682.

(14) LaPointe, A. M.; Rix, F. C.; Brookhart, M. *J. Am. Chem. Soc.* **1997**, *119*, 906−917.

(15) Broene, R. D.; Brookhart, M.; Lamanna, W. M.; Volpe, A. F. J. *J. Am. Chem. Soc.* **2005**, *127*, 17194−17195.

(16) Brookhart, M.; DeSimone, J. M.; Grant, B. E.; Tanner, M. J. *Macromolecules* **1995**, *28*, 5378−5380.

(17) Brookhart, M.; Grant, B. E. *J. Am. Chem. Soc.* **1993**, *115*, 2151−2156.

(18) Brookhart, M.; Grant, B. E.; Volpe, A. F. J. *Organometallics* **1992**, *11*, 3920−3922.

(19) Brookhart, M.; Lincoln, D. M.; Volpe, A. F. J.; Schmidt, G. F. *Organometallics* **1989**, *8*, 1212−1218.

(20) Brookhart, M.; Volpe, A. F. J. Late transition metal catalysts for olefin polymerization. EP19910200928 19910418, 1991.

(21) Brookhart, M.; Volpe, A. F. J.; Lincoln, D. M.; Horvath, I. T.; Millar, J. M. *J. Am. Chem. Soc.* **1990**, *112*, 5634−5636.

(22) Cracknell, R. B.; Orpen, A. G.; Spencer, J. L. *J. Chem. Soc., Chem. Commun.* **1984**, 326−328.

(23) Cracknell, R. B.; Orpen, A. G.; Spencer, J. L. *J. Chem. Soc., Chem. Commun.* **1986**, 1005−1006.

(24) Lenges, C. P.; Brookhart, M.; Grant, B. E. *J. Organomet. Chem.* **1997**, *528*, 199−203.

(25) Schmidt, G. F.; Brookhart, M. *J. Am. Chem. Soc.* **1985**, *107*, 1443−1444.

10.1021/om700620w CCC: \$37.00

Scheme 1. Mechanism of Co(III)-Catalyzed Olefin Hydrosilation

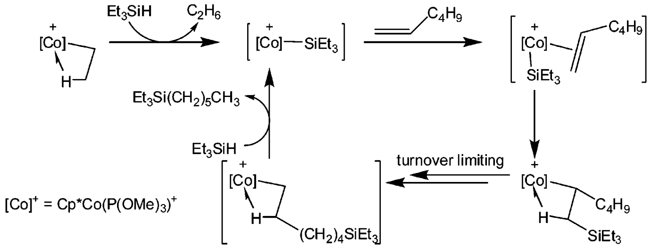

olefin hydrogenation and hydrosilation catalysts.[17,28] Chain transfer in the ethylene polymerization reaction can be achieved by cleavage of the cobalt−alkyl bond with H_2 or triethylsilane (eq 1).[16] This cleavage reaction employing H_2 is also a key step in the hydrogenation of olefins.

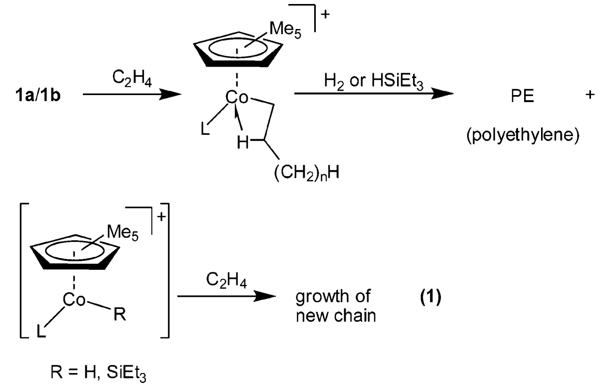

The catalytic cycle for the hydrosilation reaction is shown in Scheme 1. An unusual feature of this mechanism is that the migration of cobalt to the terminal carbon is rate-determining.[17] Again, cleavage of the cobalt−alkyl bond provides the key step in catalyst turnover.

This article reports studies aimed at elucidating the details of the cleavage of the cobalt−alkyl bonds of $[Cp^*Co(L)(CH_2CH_2\text{-}\mu\text{-}H)][B(Ar_F)_4]$ (L = $P(OCH_3)_3$, **1a**, or $P(CH_3)_3$, **1b**) with hydrogen and silanes and identifying the intermediates that result from these cleavage reactions. NMR evidence suggests that cleavage of the cobalt alkyl complexes with H_2 results in the formation of trihydride complexes that are best described as η^2-H_2/H complexes $(Cp^*(L)Co(H_2)H^+)$; the corresponding silane complexes exist as η^2-silane hydrides $(Cp^*(L)Co(HSiR_3)H^+)$. Spectroscopic as well as dynamic properties of these species provide insight into the mode of cleavage of the cobalt−alkyl bonds.

Results and Discussion

Synthesis and Characterization of $[Cp^*Co(L)(CH_2CH_2\text{-}\mu\text{-}H)][B(Ar_F)_4]$ ($Cp^* = C_5(CH_3)_5$; L = $P(OMe)_3$, 1a; L = PMe_3, 1b). As previously reported,[18,19] low-temperature protonation of the $Cp^*Co(L)(\eta^2$-ethylene) (L = $P(OMe)_3$, PMe_3) complexes with $[H(OEt_2)_2][B(Ar_F)_4]$ followed by precipitation with hexane results in the isolation of the cationic ethyl complexes **1a** and **1b**, respectively. These complexes have been characterized by low-temperature ^1H and ^{13}C NMR spectroscopy and were shown to possess β-agostic C−H bonds exhibiting C−H coupling constants of 61 Hz for **1a** and 63 Hz for **1b**. X-ray structural analysis of complexes **1a** and **1b** (see Figure 1 and Table 4) now also support the assignment as β-agostic structures, as indicated by the small $Co-C_\alpha-C_\beta$ angles (74.4(5)° for **1a** and 75.16(19)° for **1b**) and short $C_\alpha-C_\beta$ bond lengths (1.477(13) Å for **1a** and 1.462(5) Å for **1b**). These angles and bond lengths are consistent with solid-state structures of related β-agostic complexes reported by Spencer[22,29−31] and Tanner $(Cp^*Co(P(OMe)_3)(CH_2CR\text{-}\mu\text{-}H)^+$, R = C_4H_9, **1c**)[26] and with the calculated structure of $CpCo(PH_3)(CH_2CHR\text{-}\mu\text{-}H)^+$.[32]

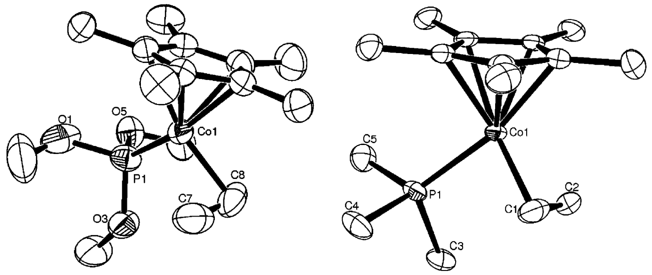

1a **1b**

Figure 1. ORTEP representations of $[Cp^*Co(P(OMe)_3)(CH_2CH_2\text{-}\mu\text{-}H)][B(Ar_F)_4]$, **1a**, and $[Cp^*Co(PMe_3)(CH_2CH_2\text{-}\mu\text{-}H)][B(Ar_F)_4]$, **1b**. The $[B(Ar_F)_4]$ anion has been omitted for clarity. Selected bond lengths (Å) and angles (deg) for **1a**: Co(1)−C(8) 1.969(7), Co(1)−C(7) 2.119, Co(1)−P(1) 2.1637(18), C(8)−C(7) 1.477(13); Co(1)−C(8)−C(7) 74.4(5), Co(1)−P(1)−O(1) 118.2(2), Co(1)−P(1)−O(3) 109.84(19), Co(1)−P(1)−O(5) 123.6(2). Selected bond lengths (Å) and angles (deg) for **1b**: Co(1)−C(1) 1.961(3), Co(1)−P(1) 2.1976(9), C(1)−C(2) 1.462(5); Co(1)−C(1)−C(2) 75.16(19), Co(1)−P(1)−C(3) 113.22(12), Co(1)−P(1)−C(4) 114.95(12), Co(1)−P(1)−C(5) 120.24(12).

Hydrogenolysis of $[Cp^*Co(L)(CH_2CH_2\text{-}\mu\text{-}H)][B(Ar_F)_4]$ ($Cp^* = C_5(CH_3)_5$; L = $P(OMe)_3$, 1a; L = PMe_3, 1b). Exposure of methylene chloride-d_2 solutions of **1a** to excess hydrogen at −30 °C results in the liberation of an equivalent of ethane and the formation of **2a** as the major product after several minutes. The upfield portion of the ^1H NMR spectrum of **2a** exhibits a broad doublet (δ −10.46, $^2J_{HP} = 29$ Hz) integrating for three protons versus the corresponding $P(OMe)_3$ and Cp* signals, indicating an empirical formula of $[Cp^*Co(P(OMe)_3)(H)_3][B(Ar_F)_4]$ for complex **2a** (eq 2). A minor additional upfield signal (δ −10.99, $^2J_{HP} = 113$ Hz) integrating for one proton is accompanied by a corresponding set of $P(OMe)_3$ and Cp* signals and has been assigned to the coordinated water complex $[Cp^*Co(P(OMe)_3)(H)(H_2O)][B(Ar_F)_4]$, **3a**, resulting from coordination of trace amounts of water present in solution. Addition of H_2 to **1a** in the presence of excess H_2O leads to quantitative formation of a single species with ^1H NMR signals matching those of the minor product **3a**, confirming the above assignment. Similar results were observed upon exposure of complex **1b** to hydrogen in methylene chloride-d_2 at −30 °C, generating complex **2b**, $[Cp^*Co(PMe_3)(H)_3][B(Ar_F)_4]$ (δ −10.70, $^2J_{HP} = 27$ Hz), as the major product and complex **3b**, $[Cp^*Co(PMe_3)(H)(H_2O)][B(Ar_F)_4]$ (δ −11.27, $^2J_{HP} = 97.5$ Hz), as a

---

(26) Tanner, M. J. Mechanistic Studies of Co(III)-Catalyzed Reactions: Living Polymerization of Ethylene. Ph.D. Thesis, University of North Carolina at Chapel Hill, Chapel Hill, 1997.

(27) Tanner, M. J.; Brookhart, M.; DeSimone, J. M. *J. Am. Chem. Soc.* **1997**, *119*, 7617−7618.

(28) Brookhart, M.; Grant, B. E.; Lenges, C. P.; Prosenc, M. H.; White, P. S. *Angew. Chem., Int. Ed.* **2000**, *39*, 1676−1679.

(29) Carr, N.; Dunne, B. J.; Orpen, A. G.; Spencer, J. L. *J. Chem. Soc., Chem. Commun.* **1988**, 926−928.

(30) Carr, N.; Mole, L.; Orpen, A. G.; Spencer, J. L. *J. Chem. Soc., Dalton Trans.* **1992**, 2653−2662.

(31) Conroy-Lewis, F. M.; Mole, L.; Redhouse, A. D.; Litster, S. A.; Spencer, J. L. *J. Chem. Soc., Chem. Commun.* **1991**, 1601−1603.

(32) Han, Y.; Deng, L.; Ziegler, T. *J. Am. Chem. Soc.* **1997**, *119*, 5939−5945.

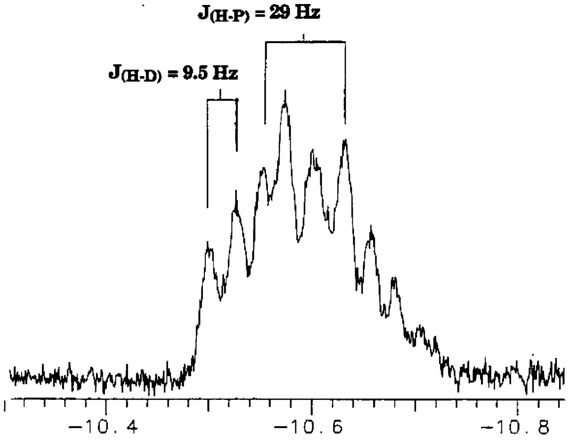

Figure 2. Upfield region of the ^1H NMR spectrum of partially deuterated **2a**.

minor species. All attempts to isolate **2a** or **2b** have led only to oils that readily decompose at room temperature.

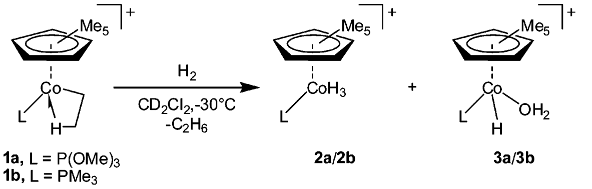

(2)

The spin−lattice relaxation time, $T_{1(min)}$, of metal-bound hydrides has been used to differentiate between classical dihydride and nonclassical η^2-H_2 structures in transition metal polyhydride complexes.[33−36] Measurement of T_1 at a variety of temperatures gives minimum values at −80 °C of 22 ms for **2a** and 52 ms for **2b**, suggesting that these complexes are likely to be η^2-H_2 complexes.[33,34,36] Since quadrapolar contributions to relaxation rates can be expected for hydrides bound to cobalt (^{59}Co $I = 7/2$, 100% natural abundance, $\gamma = 6.3015 \times 10^{-7}$ rad T^{-1} s^{-1}),[37] these $T_{1(min)}$ values are better viewed as upper limits of the relaxation rate due to dipole−dipole contributions and thus do not provide unambiguous proof of an η^2-H_2 structure.[35]

In order to better define the structural nature of these cobalt-bound hydrides, the H−D coupling constants of partially deuterated samples of **2a** and **2b** were measured by ^1H NMR spectroscopy. Removal of the H_2 atmosphere from screw cap NMR tubes containing methylene chloride-d_2 solutions of **2a** or **2b** via two freeze−pump−thaw cycles and addition of an atmosphere of deuterium gas results in the formation of an isotopic mixture of hydrides (H_3 (**2a**/**b**), H_2D (**2a**/**b**-d_1), HD_2 (**2a**/**b**-d_2), and D_3 (**2a**/**b**-d_3) isotopologues). The signals for **2a**/**b**-d_1 and **2a**/**b**-d_2 are partially obscured by the broad doublet corresponding to **2a**/**b** (shown for **2a** in Figure 2); however an H−D coupling constant of 9.5 Hz for **2a** and 9.7 Hz for **2b** could be measured. Assuming a Co(H)(η^2-H_2) structure and accounting for statistical exchange of the deuterium into terminal (Co−H) and bridging (η^2-H−H) positions, the calculated $^1J_{HD}$ coupling constants in the η^2-HD ligands are 28.5 Hz for **2a** and 29.1 Hz for **2b**. These values are fully consistent with an η^2-H_2 structural assignment.[38−43] This calculation makes the assumption that H and D statistically distribute between bridging and terminal hydride positions and there is negligible coupling between the terminal hydride and the η^2-H_2 protons.[44]

Scheme 2. Substitution of the η^2-H_2 Ligand in Co(III)−(H)(η^2-H_2)$^+$ Complexes 2a and 2b

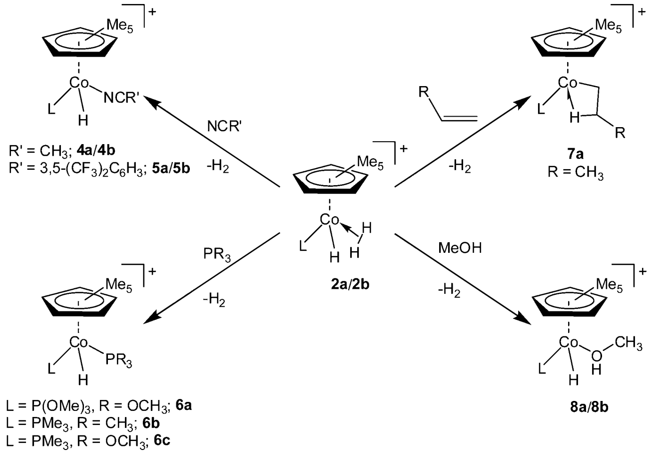

These η^2-dihydrogen complexes, Cp*Co(L)(η^2-H_2)(H)$^+$, can be added to the list of previously reported complexes possessing the general formula (C_5R_5)M(L)$(H)_3^+$ (R = H, CH_3, M = Ir[45−48] and Rh[38]). Like **2a**/**b**, all members of this family exhibit a single resonance in the upfield region of their ^1H NMR spectra at ambient temperatures. The analogous Rh complexes have been assigned an (η^2-H_2)(H) structure based on $T_{1(min)}$ measurements, H−D coupling constants, and isotopic labeling studies.[38] However, an absence of observable H−D coupling has eliminated an η^2-H_2 formulation for the reported Ir complexes, which have been characterized as classical Ir(V) trihydrides.[47,48] Arrest of the site exchange process between the unique *trans* hydride and the two equivalent *cis* hydrides has been achieved for these complexes using low-temperature ^1H NMR techniques.[47] Extremely large, temperature-dependent H−H couplings have been observed in these low-temperature spectra, a phenomenon that has been attributed to a quantum mechanical exchange process.[47−49]

Having established the structures of **2a** and **2b** as η^2-H_2 complexes, we turned to investigating the reactivity of the coordinated H_2 ligand. As shown in Scheme 2, complexes **2a**

---

(33) Crabtree, R. H. *Angew. Chem., Int. Ed. Engl.* **1993**, *32*, 789−805.

(34) Crabtree, R. H.; Hamilton, D. G. *Adv. Organomet. Chem.* **1988**, *28*, 299−338.

(35) Desrosiers, P. J.; Cai, L.; Lin, Z.; Richards, R.; Halpern, J. *J. Am. Chem. Soc.* **1991**, *113*, 4173−4184.

(36) Hamilton, D. G.; Crabtree, R. H. *J. Am. Chem. Soc.* **1988**, *110*, 4126−4133.

(37) Friebolin, H. *Basic One- and Two-Dimensional NMR Spectroscopy*, 3rd ed.; Wiley-VCH: New York, 1998; p 3.

(38) Taw, F. L.; Mellows, H.; White, P. S.; Hollander, F. J.; Bergman, R. G.; Brookhart, M.; Heinekey, D. M. *J. Am. Chem. Soc.* **2002**, *124*, 5100−5108.

(39) Heinekey, D. M.; Oldham, W. J. J. *Chem. Rev.* **1993**, *93*, 913−926.

(40) Kubas, G. J. *Acc. Chem. Res.* **1988**, *21*, 120−128.

(41) Kubas, G. J. *J. Organomet. Chem.* **2001**, *635*, 37−68.

(42) Morris, R. H. Non-classical Hydrogen Bonding along the Pathway to the Heterolytic Splitting of Dihydrogen. In *Recent Advances in Hydride Chemistry*, 1st ed.; Peruzzini, M., Poli, R., Eds.; Elsevier Science Ltd.: Amsterdam, NY, 2001; pp 1−38.

(43) Kubas, G. J. *Metal Dihydrogen and σ-Bond Complexes: Structure, Theory and Reactivity*; Kluwer Academic/Plenum Publishers: Boston, 2001; p 472.

(44) Gusev, D. G.; Kuhlman, R. L.; Renkema, K. B.; Eisenstein, O.; Caulton, K. G. *Inorg. Chem.* **1996**, *35*, 6775−6783.

(45) Gilbert, T. M.; Bergman, R. G. *J. Am. Chem. Soc.* **1985**, *107*, 3502−3507.

(46) Gilbert, T. M.; Hollander, F. J.; Bergman, R. G. *J. Am. Chem. Soc.* **1985**, *107*, 3508−3516.

(47) Heinekey, D. M.; Hinkle, A. S.; Close, J. D. *J. Am. Chem. Soc.* **1996**, *118*, 5353−5361.

(48) Heinekey, D. M.; Millar, J. M.; Koetzle, T. F.; Payne, N. G.; Zilm, K. W. *J. Am. Chem. Soc.* **1990**, *112*, 909−919.

(49) Sabo-Etienne, S.; Chaudret, B. *Chem. Rev.* **1998**, *98*, 2077−2091.

Table 1. ^{1}H NMR Data for Cp*Co(L)(H)(L′)$^+$ Complexes 2−6, 8, and 10

complex	δ Co−H (ppm)	$^2J_{HP}$ (Hz)
$Cp^*Co(P(OMe)_3)(H)(\eta^2\text{-}H_2)^+$ **2a**^{a}	−10.46, d	29
$Cp^*Co(PMe_3)(H)(\eta^2\text{-}H_2)^+$ **2b**^{a}	−10.70, d	27
$Cp^*Co(P(OMe)_3)(H)(OH_2)^+$ **3a**^{a}	−10.99, d	113
$Cp^*Co(PMe_3)(H)(OH_2)^+$ **3b**^{a}	−11.27, d	98
$Cp^*Co(P(OMe)_3)(H)(NCCH_3)^+$ **4a**^{a}	−12.54, d	110
$Cp^*Co(PMe_3)(H)(NCCH_3)^+$ **4b**^{a}	−13.58, d	101
$Cp^*Co(P(OMe)_3)(H)(NCAr_F)^+$ **5a**^{a}	−12.11, d	109
$Cp^*Co(PMe_3)(H)(NCAr_F)^+$ **5b**^{a}	−13.14, d	99
$Cp^*Co(P(OMe)_3)_2(H)^+$ **6a**^{b}	−14.29, t	81
$Cp^*Co(PMe_3)_2(H)^+$ **6b**^{a}	−16.60, t	80
$Cp^*Co(P(OMe)_3)(PMe_3)(H)^+$ **6c**^{a}	−15.30, dd	76 and 86
$Cp^*Co(P(OMe)_3)(H)(CH_3OH)^+$ **8a**^{c}	−11.52, d	121
$Cp^*Co(PMe_3)(H)(CH_3OH)^+$ **8b**^{a}	−11.63, d	108
$Cp^*Co(P(OMe)_3)(H)_2$ **10a**^{a}	−17.23, d	98
$Cp^*Co(PMe_3)(H)_2$ **10b**^{a}	−18.09, d	89

^{a} CD_2Cl_2 solution at −30 °C at 500 MHz. ^{b}CD_2Cl_2 solution at 25 °C at 300 MHz. ^{c}CD_2Cl_2 solution at 20 °C at 500 MHz.

and **2b** can be considered a convenient source of the $[Cp^*CoL(H)]^+$ fragment. Addition of 2 equiv of acetonitrile to solutions of **2a** or **2b** quantitatively generates the corresponding $[Cp^*Co(L)(H)(NCCH_3)][B(Ar_F)_4]$ complexes **4a** and **4b**, while addition of ∼1 equiv of 3,5-bis(trifluoromethyl)benzonitrile to solutions of **2a** or **2b** quantitatively generates the corresponding $[Cp^*Co(L)(H)(NC(3,5\text{-}(CF_3)_2C_6H_3))][B(Ar_F)_4]$ complexes **5a** and **5b**. Similarly, addition of 1 equiv of $P(OMe)_3$ to **2a** or PMe_3 to **2b** quantitatively generates the corresponding bisphosphite and bisphosphine hydride complexes, **6a** and **6b**, respectively. Also, addition of 1 equiv of $P(OMe)_3$ to **2b** results in the formation of the mixed phosphine/phosphite hydride complex **6c**. Consistent with our findings that these Co(III) complexes function as olefin hydrogenation catalysts, addition of an olefin such as propene to **2a** generates the previously reported β-agostic propyl complex, **7a** ($R = CH_3$).[19] Finally, addition of 3 equiv of methanol to a solution of **2a** or **2b** quantitatively generates the corresponding O-bound methanol hydride adducts **8a** and **8b**, as evidenced by the observation in the ^{1}H NMR spectrum of a methyl doublet (**8a**: δ 3.00, $^3J_{HH} = 4.5$ Hz; **8b**: δ 2.91 broad doublet) and a 1H quartet (**8a**: δ 3.94 broad quartet; **8b**: δ 3.94 broad quartet) corresponding to coordinated methanol. The chemical shift of the O*H* of bound methanol (δ 3.94) should be a good model for the chemical shifts of bound OH_2 in **3a** and **3b**; however, no signals for **3a** and **3b** are observed in this range. Their absence may be the result of exchange broadening. The ^{1}H NMR data for the Co-H signals of complexes **2**−**6** and **8** and **10** are presented in Table 1 along with the relevant J_{PH} coupling constants. The low J_{PH} coupling constants for the cobalt η^2-H_2 monohydride complexes **2a** and **2b** (29 and 27 Hz) relative to the monohydride complexes (**3a**/**3b**−**6a**/**6b**, **8a**/**8b**) no doubt arise from averaging of a high J_{PH} for the terminal hydride with a low J_{PH} value for the η^2-H_2 ligand. Assuming a J_{PH} of ca. 80−90 Hz for the terminal hydride, the J_{PH} for the η^2-H_2 ligand must be near zero. Upon addition of methyl acrylate to a solution of **2a** at −30 °C, hydrogen is displaced and products from both 1,2- and 2,1-insertion of acrylate into the Co−H bond result. Rather than agostic species analogous to **7a**, complexes **9a** and **9a′** (initial ratio = 1:11) are produced, which exhibit chelation of the carbonyl oxygen to complete the 18-electron configuration at Co(III) (eq 3). Structures similar to both **9a** and **9a′** are well-precedented.[50−54] The methine hydrogen of **9a′** appears as a quartet at δ 3.90 with a corresponding methyl doublet at δ 1.15, while the methylene hydrogens of the 1,2-insertion product **9a** appear as four separate multiplets between 2.2 and 2.9 ppm, indicating two sets of diastereotopic methylene groups as a result of chelation of the carbonyl group and the chiral center at cobalt. It is likely the carbonyl group is coordinated to Co as shown in **9a′**; however, there is no spectroscopic evidence to support such an assumption. The alternative structure would involve an oxa-π-allyl structure, i.e., coordination as an enolate.[55,56]

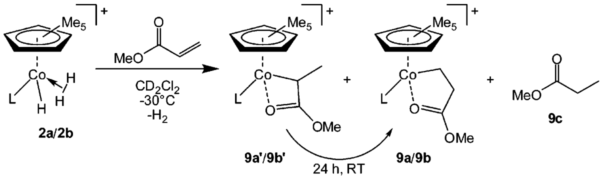

(3)

Over a period of 24 h at room temperature, this isomeric mixture converts completely to **9a**, which can then be isolated as a stable red-brown solid. Concomitant formation of methyl propionate **9c** is observed by ^{1}H NMR spectroscopy, resulting from hydrogenation of methyl acrylate by the H_2 released upon olefin coordination. Insertion of methyl acrylate into the Co−H bond of **2b** results in a similar mixture of regioisomeric products, which convert to the 1,2-insertion product **9b**.

The source of the methyl propionate appears to be hydrogenolysis of the 2,1-insertion product **9a′**. Chelate **9a** is unreactive toward hydrogen, and furthermore the apparently tight chelate interaction is not disrupted by strong ligands including acetonitrile, PMe_3, and $P(OMe)_3$. While one could envision a mechanism of conversion of **9a′** to **9a** involving continual hydrogenolysis of **9a′** and ultimately funneling all product to the unreactive **9a**, the amount of hydrogen present and the amount of methyl propionate formed are inconsistent with such a process. Furthermore, isomerization of **9a′** to **9a** occurs at a similar rate when hydrogen is completely removed from the −30 °C solution via three freeze−pump−thaw cycles. Thus, conversion of **9a′** to **9a** is proposed to occur via a standard β-elimination, olefin rotation, reinsertion mechanism. As in similar cases,[50−52,54,57] the five-membered chelates (**9a**/**9b**) are thermodynamically favored over the four-membered chelates (**9a′**/**9b′**).

Single crystals of **9a** suitable for X-ray diffraction analysis were obtained by vapor diffusion of pentane into a concentrated solution of isolated **9a** in toluene. An ORTEP representation and key bond distances and angles for **9a** are shown in Figure 3 (crystallographic data are summarized in Table 4). The carbonyl group is coordinated to Co through the oxygen (Co(1)−O(4) = 1.974(3) Å), as was suggested on the basis of ^{1}H NMR data.

In addition to H_2 substitution and olefin insertion chemistry, **2a** and **2b** also react as acids upon exposure to amine bases, as is shown in eq 4. Addition of ∼1 equiv of triethylamine to

---

(50) Brookhart, M.; Hauptman, E. *J. Am. Chem. Soc.* **1992**, *114*, 4437−4439.

(51) Brookhart, M.; Sabo-Etienne, S. *J. Am. Chem. Soc.* **1991**, *113*, 2777−2779.

(52) Hauptman, E.; Sabo-Etienne, S.; White, P. S.; Brookhart, M.; Garner, J. M.; Fagan, P. J.; Calabrese, J. C. *J. Am. Chem. Soc.* **1994**, *116*, 8038−8060.

(53) Johnson, L.; Bennett, A.; Dobbs, K.; Hauptman, E.; Ionkin, A.; Ittel, S.; McCord, E.; McLain, S.; Radzewich, C.; Yin, Z.; Wang, L.; Wang, Y.; Brookhart, M. *PMSE Preprints* **2002**, *86*, 319.

(54) Yi, C. S.; Liu, N. *J. Organomet. Chem.* **1998**, *553*, 157−161.

(55) Burkhardt, E. R.; Doney, J. J.; Bergman, R. G.; Heathcock, C. H. *J. Am. Chem. Soc.* **1987**, *109*, 2022−2039.

(56) Doney, J. J.; Bergman, R. G.; Heathcock, C. H. *J. Am. Chem. Soc.* **1985**, *107*, 3724−3726.

(57) Gottfried, A. C.; Brookhart, M. *Macromolecules* **2003**, *36*, 3085−3100.

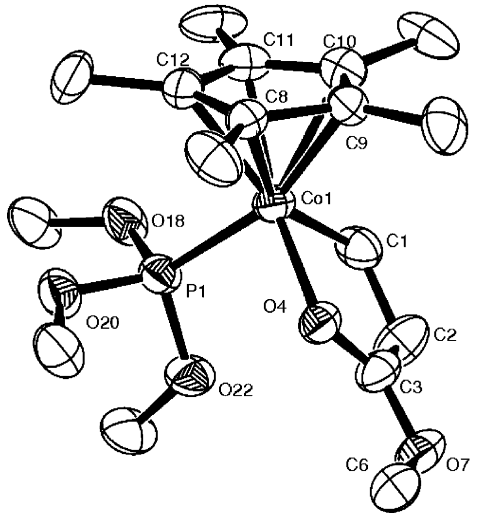

Figure 3. ORTEP representation of [Cp*Co(P(OMe)$_3$)(CH$_2$CH$_2$C(O)OCH$_3$)][B(Ar$_F$)$_4$], **9a**. The [B(Ar$_F$)$_4$] anion has been omitted for clarity. Selected bond lengths (Å) and angles (deg): Co(1)−C(1) 2.013(6), C(1)−C(2) 1.511(8), C(2)−C(3) 1.488(8), C(3)−O(4) 1.232(6), Co(1)−O(4) 1.974(3), C(3)−O(7) 1.310(6), O(7)−C(6) 1.447(7), Co(1)−P(1) 2.1339(16), Co(1)−C(8) 2.135(7), Co(1)−C(9) 2.117(8), Co(1)−C(10) 2.077(9), Co(1)−C(11) 2.037(8), Co(1)−C(12) 2.123(8); O(4)−Co(1)−C(1) 84.9(2), Co(1)−C(1)−C(2) 108.4(4), C(1)−C(2)−C(3) 110.5(5), C(2)−C(3)−O(4) 121.6(5), C(3)−O(4)−Co(1) 114.2(3), C(2)−C(3)−O(7) 116.7(5), C(3)−O(7)−C(6) 116.8(4), Co(1)−P(1)−O(18) 114.36(16), Co(1)−P(1)−O(20) 118.79(17), Co(1)−P(1)−O(22) 111.71(16).

methylene chloride-d_2 solutions of **2a** and **2b** quantitatively generates the neutral Co(III) dihydride complexes **10a** and **10b**. Similar heterolytic cleavage of η^2-H$_2$ ligands has been reported by Crabtree[58] for the deprotonation of [IrH(η^2-H$_2$)(bq)(PPh$_3$)$_2$]$^+$ (bq = benzoquinone) by alkyl lithium reagents and by Heinekey[59] for the deprotonation of [CpRu(dmpe)(η^2-H$_2$)]$^+$ (dmpe = 1,2-bis(dimethylphosphino)ethane) by triethylamine to generate the corresponding Ru−H complex.

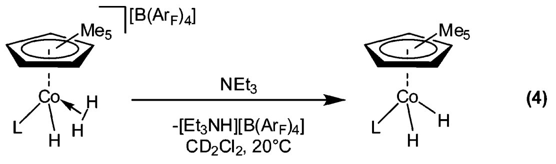

2a/2b 10a/10b (4)

Silanolysis of [Cp*Co(L)(CH$_2$CH$_2$-μ-H)][B(Ar$_F$)$_4$] (Cp* = C$_5$(CH$_3$)$_5$; L = P(OMe)$_3$, 1a; L = PMe$_3$, 1b). Reaction of **1a** with triethylsilane followed a less straightforward route relative to the hydrogenolysis reaction. Monitoring the reaction of **1a** with Et$_3$SiH (5 equiv) at 25 °C by ^{1}H NMR spectroscopy showed the formation of two major cobalt hydride products and the liberation of 1 equiv of ethane. The first of these, **11a**, exhibited a doublet (δ −13.30, $^2J_{HP}$ = 51 Hz) that was initially believed to correspond to Cp*Co(P(OMe)$_3$)(SiEt$_3$)$_2$(H)$^+$ (**B**, Scheme 3), the expected product from reaction of Cp*Co(P(OMe)$_3$)(SiEt$_3$)$^+$ (intermediate **A**, Scheme 3) with an additional equivalent of silane. However, recognizing that cationic metal silyl complexes are highly electrophilic and extremely sensitive to water, the possibility that **11a** resulted from hydrolysis of Cp*Co(P(OMe)$_3$)(SiEt$_3$)$_2$(H)$^+$ (**B**) and had the formula Cp*Co(P(OMe)$_3$)(SiEt$_3$)(H)$_2$$^+$ (**D**, Scheme 3) was also considered. Due to overlapping metal hydride signals between **11a** and the other major product, distinguishing between these possible structures on the basis of signal integration was not possible. Prolonged reaction times lead to signals due to **2a** and **2b**, indicating further hydrolysis of the Co−Si moiety.

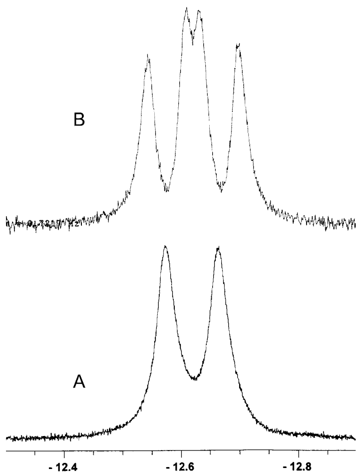

Figure 4. (A) Upfield region of the ^{1}H NMR spectrum of Cp*Co(P(OMe)$_3$)(H)$_2$(SiPhMeH)$^+$ (**14a**) at −30 °C showing the Co−H signal (δ −12.60, $^2J_{HP}$ = 46.5 Hz). (B) ^{29}Si satellites obtained after the ^{1}H/^{29}Si HMQC of **14a** (δ −12.60, $^1J_{SiH(observed)}$ = 33.5 Hz, $^2J_{HP}$ = 46.5 Hz).

Scheme 3. Reaction of 1a and Et$_3$SiH

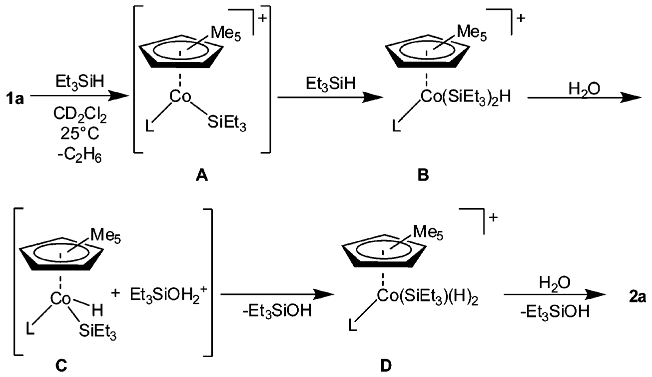

The η^2-dihydrogen hydride complex **2a** serves as a convenient source of Cp*Co(P(OMe)$_3$)(H)$^+$ (*vide supra*) and as such is a logical starting point for the independent synthesis of compounds with the general formula Cp*Co(P(OMe)$_3$)(SiEt$_3$)(H)$_2$$^+$. Addition of a slight excess of Et$_3$SiH to a CD$_2$Cl$_2$ solution of **2a** resulted in the loss of hydrogen and quantitative formation of a species with ^{1}H NMR signals matching those of **11a**. The Co−H signal integrates for two protons versus the corresponding Cp* and P(OMe)$_3$ signals, consistent with the formula Cp*Co(P(OMe)$_3$)(SiEt$_3$)(H)$_2$$^+$. Close examination of the Co−H signal (δ −13.30) revealed the presence of ^{29}Si satellites (I = 1/2, 4.7% natural abundance);[37] however due to short $T_{1(min)}$ values and the quadrupole moment of ^{59}Co, which broadens the hydride signal, these satellites are not sufficiently resolved to obtain accurate ^{29}Si−^{1}H coupling constants. Enhancement of the ^{29}Si satellites was achieved using a 1D ^{1}H/^{29}Si HMQC experiment (500.13 MHz), providing a ^{29}Si−^{1}H coupling constant of 29 Hz (shown for the PhMeSiH$_2$ complex **14a** in Figure 4). Knowing this coupling constant, we were also able to employ a ^{29}Si{^{1}H} DEPT 45 experiment to obtain a ^{29}Si chemical shift of δ 20.9 ($^2J_{SiP}$ = 11 Hz) relative to Me$_4$Si (δ 0.00).

---

[58] Crabtree, R. H.; Lavin, M. *J. Chem. Soc., Chem. Commun.* **1985**, 794−795.

[59] Chinn, M. S.; Heinekey, D. M. *J. Am. Chem. Soc.* **1987**, *109*, 5865−5867.

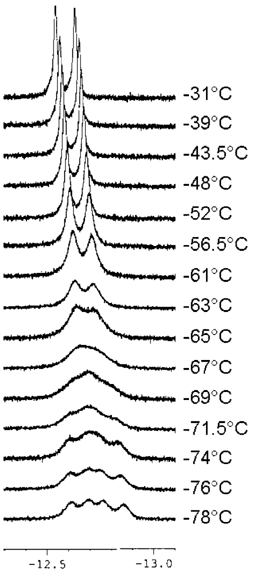

Figure 5. Variable-temperature ^{1}H NMR of **14a**.

The same procedure can be used to generate *in situ* a variety of complexes with the general formula Cp*Co(L)(SiR$_3$)H$_2$$^+$ starting from **2a** or **2b** (eq 5). Addition of Ph$_2$SiH$_2$, PhSiH$_3$, and Ph(Me)SiH$_2$ to **2a** generates the corresponding phosphite complexes **12a**, **13a**, and **14a**, respectively; while addition of Et$_3$SiH, Ph$_2$SiH$_2$, PhSiH$_3$, and Ph(Me)SiH$_2$ to **2b** quantitatively generates the corresponding phosphine complexes **11b**, **12b**, **13b**, and **14b**. Complexes **12**−**14** contain terminal Si−H bonds which are not coordinated to cobalt and do not undergo interchange with the metal-bound hydrides. They exhibit slightly higher ^{29}Si−^{1}H coupling constants (216−222 Hz), relative to the ^{29}Si−^{1}H coupling constants in the free silanes (Ph$_2$SiH$_2$: $^{1}J_{\mathrm{SiH}} = 200$ Hz, PhSiH$_3$: $^{1}J_{\mathrm{SiH}} = 200$ Hz, PhMeSiH$_2$: $^{1}J_{\mathrm{SiH}} = 193$ Hz).

The ^{1}H NMR spectrum of a CD$_2$Cl$_2$ solution of **14a** below −31 °C shows broadening of the Co−H doublet at δ −12.60 (Figure 5), while complete decoalescence into two doublets is observed at −78 °C. By contrast, the Co−H signals for **11a**−**13a** do not exhibit any appreciable broadening at −80 °C. ^{1}H NMR data for the Co−H signals of complexes **11**−**14** are presented in Table 2 along with the relevant ^{31}P and ^{29}Si coupling constants.

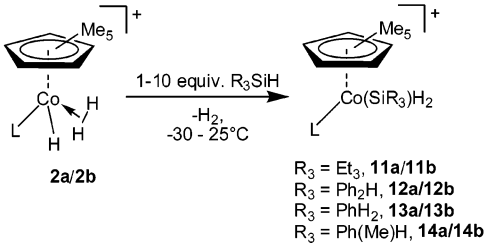

(5)

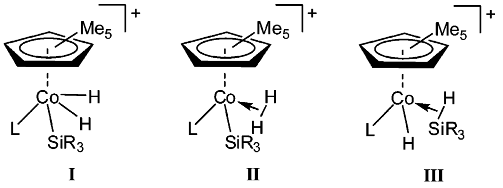

Figure 6. Possible structures for Cp*Co(L)(SiR$_3$)H$_2$$^+$.

Three structures having the formula Cp*Co(P(OMe)$_3$)(SiR$_3$)(H)$_2$$^+$ were considered for complex **11a** (Figure 6): a classical Co(V) silyl dihydride structure Cp*Co(P(OMe)$_3$)(SiR$_3$)(H)$_2$$^+$ (**I**), a Co(III) silyl η^2-dihydrogen structure Cp*Co(P(OMe)$_3$)(SiR$_3$)(η^2-H$_2$)$^+$ (**II**), and a Co(III) η^2-silane hydride structure Cp*Co(P(OMe)$_3$)(η^2-HSiR$_3$)(H)$^+$ (**III**). The silyl η^2-H$_2$ structure **II** was ruled out using a deuterium labeling experiment. In structure **II** the hydrogen atoms always reside in an η^2-H$_2$ ligand, and thus in the d_1-labeled complexes, J_{HD} values of ca. 30 Hz should be observed. Addition of Ph$_2$SiH$_2$ to samples of **2a-*d$_n$*** to form Cp*Co(P(OMe)$_3$)(SiPh$_2$H)(D)$_{2-n}$(H)$_n$$^+$, **12a-*d$_n$***, exhibited a decrease in the intensity of the Co−H signal; however no H−D coupling was observed. The presence of deuterium in the terminal Co−H position as indicated by the decreased signal intensity and the lack of H−D coupling clearly indicate that the silyl η^2-H$_2$ structure **II** is not the correct structure of **12a**.

Distinguishing between the classical silyl dihydride structure **I** and the η^2-silane hydride structure **III** can be accomplished using the ^{29}Si−^{1}H coupling constants. The J_{SiH} values for η^2-silane complexes typically fall in the range 40−160 Hz, while J_{SiH} values between terminal hydride and terminal silyl substituents are very much smaller.[60−70] ^{1}H NMR spectra of complexes **11**−**14** exhibit a single cobalt−hydride resonance of intensity 2H down to −80 °C (complexes **14a** and **14b** exhibit dynamic behavior below −30 °C, which will be discussed below) and observed ^{29}Si−^{1}H coupling constants in the range 29−32 Hz (see Table 2), implying dynamic behavior whereby terminal (i.e., Co−H) and bridging (i.e., η^2-H−Si) hydrides undergo site exchange.[71−73] As a result, the observed ^{29}Si−^{1}H coupling constants represent a time-averaged value between the terminal (i.e., $^{2}J_{\mathrm{SiH}}$) and bridging (i.e., $^{1}J_{\mathrm{SiH}}$) hydrides.[74,75] Under the assumption that there is no observed coupling between the terminal hydrides and ^{29}Si (i.e., $^{2}J_{\mathrm{SiH}} = 0$ Hz),[28,75] the ^{29}Si−^{1}H coupling constant ($^{1}J_{\mathrm{SiH}}$) is calculated to be 58 Hz for **11a** and 58 Hz for **11b**, in good agreement with expected values.[63,67−69] The observed values of ^{29}Si−^{1}H coupling constants for complexes **12**−**14** are displayed in Table 2 and range from 29 to 34 Hz, implying η^2-Si−H structures for all of these species with $^{1}J_{\mathrm{SiH}}$ values of 58−68 Hz.

The ^{29}Si{^{1}H} NMR spectra of these η^2-silane complexes were also examined and the chemical shifts of **11**−**14** along with

---

(60) No ^{29}Si−^{1}H coupling was observed in the related neutral dihydridodisilyl Co(V) complexes: See ref 28.

(61) Bart, S. C.; Lobkovsky, E.; Chirik, P. J. *J. Am. Chem. Soc.* **2004**, *126*, 13794−13807.

(62) Colomer, E.; Corriu, R. J. P.; Marzin, C.; Vioux, A. *Inorg. Chem.* **1982**, *21*, 368−373.

(63) Corey, J. Y.; Braddock-Wilking, J. *Chem. Rev.* **1999**, *99*, 175−292.

(64) Hashimoto, H.; Hayashi, Y.; Aratani, I.; Kabuto, C.; Kira, M. *Organometallics* **2002**, *21*, 1534−1536.

(65) Karshtedt, D.; Bell, A. T.; Tilley, T. D. *Organometallics* **2006**, *25*, 4471−4482.

(66) Luo, X.; Kubas, G. J.; Bryan, J. C.; Burns, C. J.; Unkefer, C. J. *J. Am. Chem. Soc.* **1994**, *116*, 10312−10313.

(67) Nikonov, G. I. *Adv. Organomet. Chem.* **2005**, *53*, 217−309.

(68) Schneider, J. J. *Angew. Chem., Int. Ed.* **1996**, *35*, 1068−1075.

(69) Schubert, U. *Adv. Organomet. Chem.* **1990**, *30*, 151−187.

(70) Yong, L.; Hofer, E.; Wartchow, R.; Butenschön, B. *Organometallics* **2003**, *22*, 5463−5467.

(71) Atheaux, I.; Delpech, F.; Donnadieu, B.; Sabo-Etienne, S.; Chaudret, B.; Hussein, K.; Barthelat, J.; Braun, T.; Duckett, S. B.; Perutz, R. N. *Organometallics* **2002**, *21*, 5347−5357.

(72) Hussein, K.; Marsden, C. J.; Barthelat, J.; Rodriguez, V.; Conejero, S.; Sabo-Etienne, S.; Donnadieu, B.; Chaudret, B. *J. Chem. Soc., Chem. Commun.* **1999**, 1315−1316.

(73) Lachaize, S.; Sabo-Etienne, S. *Eur. J. Inorg. Chem.* **2006**, 2115−2127.

(74) Ng, S. M.; Lau, C. P.; Fan, M.; Lin, Z. *Organometallics* **1999**, *18*, 2484−2490.

(75) Taw, F. L.; Bergman, R. G.; Brookhart, M. *Organometallics* **2004**, *23*, 886−890.

Scheme 4. Possible Hydride Exchange Pathways in η^2-Silane Complexes

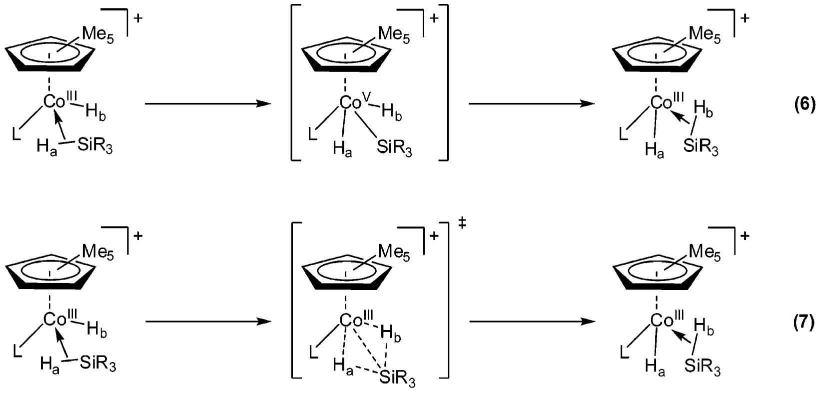

Table 2. ^{1}H NMR Data for Co(III) Complexes 11−14

complex	δ Co−H (ppm)	$^2J_{HP}$ (Hz)	$^1J_{SiH(obsd)}$[a] (Hz)
$Cp^*Co(P(OMe)_3)(H)(\eta^2\text{-}HSiEt_3)^+$, **11a**[b]	−13.30, d	51	29
$Cp^*Co(PMe_3)(H)(\eta^2\text{-}HSiEt_3)^+$, **11b**[c]	−13.96, d	45	29
$Cp^*Co(P(OMe)_3)(H)(\eta^2\text{-}H_2SiPh_2)^+$, **12a**[d]	−12.14, d	46	31.5
$Cp^*Co(PMe_3)(H)(\eta^2\text{-}H_2SiPh_2)^+$, **12b**[d]	−13.06, d	41	30
$Cp^*Co(P(OMe)_3)(H)(\eta^2\text{-}H_3SiPh)^+$, **13a**[b]	−12.34, d	44	29
$Cp^*Co(PMe_3)(H)(\eta^2\text{-}H_3SiPh)^+$, **13b**[d]	−13.14, d	43.5	29
$Cp^*Co(P(OMe)_3)(H)(\eta^2\text{-}H_2Si(Me)Ph)^+$, **14a**[d]	−12.60, d	46.5	33.5
$Cp^*Co(PMe_3)(H)(\eta^2\text{-}H_2Si(Me)Ph)^+$, **14b**[d]	−13.15, d	44.5	28.5

[a] Calculated values of the ^{29}Si−^{1}H coupling constants in the range 58−68 Hz, $^1J_{SiH(calc.)}$, are obtained by doubling the $^1J_{SiH(obsd)}$ values reported here. [b] CD_2Cl_2 solution at 25 °C at 400 MHz. [c] CD_2Cl_2 solution at −19 °C at 500 MHz. [d] CD_2Cl_2 solution at −30 °C at 500 MHz.

Table 3. ^{29}Si{^{1}H} NMR Data for Co(III) Complexes 11−14[a]

complex	δ ^{29}Si (ppm)	$^2J_{SiP}$ (Hz)	Δ[b] (ppm)
$Cp^*Co(P(OMe)_3)(H)(\eta^2\text{-}HSiEt_3)^+$, **11a**	20.9, d	10.9	20.6
$Cp^*Co(PMe_3)(H)(\eta^2\text{-}HSiEt_3)^+$, **11b**	20.7, br		20.4
$Cp^*Co(P(OMe)_3)(H)(\eta^2\text{-}H_2SiPh_2)^+$, **12a**	−2.5, d	13.0	30.6
$Cp^*Co(PMe_3)(H)(\eta^2\text{-}H_2SiPh_2)^+$, **12b**	0.7, d	14.0	33.8
$Cp^*Co(P(OMe)_3)(H)(\eta^2\text{-}H_3SiPh)^+$, **13a**	−28.4, br		31.0
$Cp^*Co(PMe_3)(H)(\eta^2\text{-}H_3SiPh)^+$, **13b**	−26.7, d	14.0	32.7
$Cp^*Co(P(OMe)_3)(H)(\eta^2\text{-}H_2Si(Me)Ph)^+$, **14a**	−8.9, d	12.3	26.7
$Cp^*Co(PMe_3)(H)(\eta^2\text{-}H_2Si(Me)Ph)^+$, **14b**	−9.0, d	13.5	26.6

[a] CD_2Cl_2 solution at −30 °C at 99.36 MHz (relative to external $(CH_3)_4Si$ at $\delta = 0.00$). [b] Δ (ppm) $= \delta_{coord} - \delta_{free}$. ^{29}Si{^{1}H} NMR δ_{free} $Et_3SiH = 0.29$, $PhSiH_3 = -59.4$, $Ph_2SiH_2 = -33.1$, $PhMeSiH_2 = -35.6$.

the change in chemical shift upon η^2-coordination to the metal (Δ (ppm) $= \delta_{coord} - \delta_{free}$) are displayed in Table 3. Regardless of the phosphorus ligand employed, the chemical shifts of the η^2-coordinated silanes are shifted approximately 20−30 ppm downfield relative to the uncoordinated silanes, consistent with reported ^{29}Si chemical shifts of other η^2-silane complexes.[74] The limited number of examples containing ^{29}Si NMR data of Co-silyl complexes exhibit ^{29}Si chemical shifts that are shifted significantly downfield (>50 ppm) relative to the uncoordinated silanes. Related Co(I) silyl complexes, $(CO)_3(L)Co(SiEt_3)$, reported by Cutler exhibit ^{29}Si chemical shifts of δ 51.9 (L = PPh_2Me) and 52.9 (L = PPh_3),[76] while the neutral silyl hydride complex $CpCo(C_2H_4)(SiEt_3)H$ recently reported by Perutz exhibits a ^{29}Si chemical shift of δ 38.9 (relative to external $(CH_3)_4Si$ at δ 0.00).[77] (Note that this neutral, Co(III) species exists as the oxidative addition adduct, not the Co(I) η^2-silane complex.)

As in the trihydride cases, Rh and Ir silyl dihydride analogues of **11**−**14** have been reported with Ph_3SiH. As expected on the basis of the trihydride structures, the Rh complexes, for example, $Cp^*(PMe_3)Rh(H)(\eta^2\text{-}HSiPh_3)^+$,[75] exist as Rh(III) η^2-silane hydrides with structures analogous to **12a**/**b**, whereas the Ir systems exist as classical Ir(V) aryl silyl hydrides as a result of *ortho*-C−H activation of a Si-Ph substituent.[2] Along with complexes **1a**/**b** and **2a**/**b**, η^2-coordination of a Si−H bond to a Cp*Co(L)(R)$^+$ fragment completes a series of compounds featuring η^2-$C_\beta H$, η^2-H_2, and η^2-SiH ligands.[41] One noteworthy aspect of these Co-(η^2-silane) cations is that the Si center is extremely electrophilic. Despite the most rigorous attempts to dry NMR solvents, the presence of **2a**/**b** in samples of **11**−**14** generated by addition of silane to **1a**/**b** indicates that these species react rapidly with trace amounts of moisture. This is reminiscent of the acute moisture sensitivity of $Cp^*Co(L)(CH_2CH(SiR_3)\text{-}\mu\text{-}H)^+$, a previously reported compound that likewise hydrolyzes to give **1a**/**b**.[17]

Hydride Exchange Mechanisms in [Cp*Co(L)(H)(η^2-HSiR$_3$)][B(Ar$_F$)$_4$] Complexes 11−14. The observation of a single Co−H signal in the ^{1}H NMR spectra of η^2-silane hydride complexes **11**−**13** down to −80 °C shows that the terminal (i.e., Co−H) and bridging (i.e., η^2-H−Si) hydrides are exchanging rapidly on the NMR time scale with barriers certainly less than ca. 7−8 kcal/mol. Two possible mechanisms for this dynamic process can be envisioned that exchange hydrides between bridging and terminal positions. The first of these processes (eq 6, Scheme 4) involves full cleavage of the μ-H_a−Si bond and formation of a Co(V) silyl dihydride in which the two hydrides are equivalent. The second mechanism, which we favor, involves what can be described as a "silyl slide", a process in which there is no increase in Co−Si bonding as Si "slides" from one hydrogen to the adjacent one and a formal Co(V) oxidation state is avoided (eq 7, Scheme 4). This latter mechanism has been invoked in many similar processes involving late metals.[14,78] It has been analyzed and discussed in detail by Perutz and Sabo-Etienne, who have proposed that such a mechanism applies to σ-bond metathesis reactions of late metal complexes, a process they term σ-complex-assisted metathesis (σ-CAM).[78]

The dynamic behavior of **14a** is somewhat more complex than that of **11**−**13**. Coordination of the prochiral silane, $PhMeSiH_2$, results in generation of both a chiral Co center and a chiral Si center, and thus two diastereomers can be formed, **14a** and **14a′**, as shown in Scheme 5. A rapid silyl slide process interconverts diastereomers and will interconvert H_a and $H_{a'}$ and H_b and $H_{b'}$ in the two diastereomers, but will not scramble H_a/$H_{a'}$ with H_b/$H_{b'}$. Yet at −31 °C only one signal is seen for the

---

[76] Gregg, B. T.; Cutler, A. R. *Organometallics* **1992**, *11*, 4276−4284.

[77] Ampt, K. A. M.; Duckett, S. B.; Perutz, R. N. *Dalton Trans.* **2007**, 2993−2996.

[78] Perutz, R. N.; Sabo-Etienne, S. *Angew. Chem., Int. Ed.* **2007**, *46*, 2578−2592.

Scheme 5. Interconversion of Diastereomers 14a and 14a′

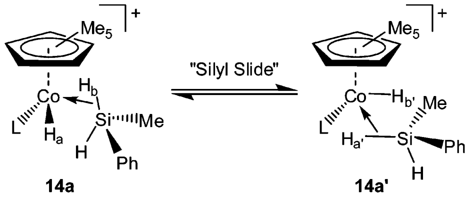

average of all four hydrogens (Figure 5, one doublet, average $J_{HP} = 46.5$ Hz). At low temperatures it is evident that the signal decoalesces into two doublets of nearly equal intensity, which we assign to $H_a/H_{a'}$ and $H_b/H_{b'}$ of the rapidly interconverting diastereomers.

We propose that the interconversion of $H_a/H_{a'}$ with $H_b/H_{b'}$ occurs through the intermediacy of an η^2-dihydrogen complex, as shown for one diastereomer in Scheme 6. Rotation of the silane brings H_a and H_b into a "*cis*" orientation. A hydrogen "slide" (analogous to the silyl slide) results in formation of a η^2-H_2 silyl species, **15a**. Rotation of the η^2-H_2 ligand interchanges H_a and H_b and results in exchange of H_a and H_b in diastereomer **14a**. A similar process can occur in **14a′**, and coupled with a rapid silyl slide that interchanges diastereomers, all four hydrogens undergo site exchange. Since the η^2-H_2 silyl isomer is higher in energy than the η^2-silane hydride isomer, the barrier for this dynamic process is now in a range measurable by NMR spectroscopy. The overall barrier for the process can be roughly estimated from the coalescence temperature (ca. −75 °C) to be ca. 9.4 kcal/mol. (It is significant to note here that the terminal Si−H does not scramble with the bridging Si−H on an NMR time scale. A similar feature applies to **12a**/**12b** and **13a**/**13b**.)

Cobalt−Alkyl Bond Cleavage Mechanism. The spectroscopic characterization of complexes **2a**/**b** and **11**−**14** as nonclassical structures $[Cp^*Co(L)(H)(\eta^2\text{-}H_2)][B(Ar_F)_4]$ and $[Cp^*Co(L)(H)(\eta^2\text{-}HSiR_3)][B(Ar_F)_4]$ and the dynamic processes these species exhibit provide insight into the mechanism of the cleavage of the metal alkyl bond in Co alkyl agostic complexes by silanes and H_2, key steps in hydrogenation and hydrosilation (see Scheme 1).[17] The agostic complex is assumed to react with H_2 or silanes to yield initially the η^2-H_2 or η^2-silane complexes **16** and **17** (eqs 8 and 9, Scheme 7). Cleavage of the cobalt alkyl bond likely occurs as shown in Scheme 7, where an η^2-alkane complex is formed by the same mechanism as proposed for the dynamic processes studied above followed by loss of alkane, thus avoiding a formal Co(V) intermediate. This overall process conforms exactly to the σ-CAM process discussed by Perutz and Sabo-Etienne and is assumed to operate in a variety of catalytic processes including the activation of dihydrogen,[79,80] silanes,[81] boranes,[82,83] and alkanes.[79,80,84]

Summary

Addition of H_2 to electrophilic Co(III) agostic alkyl complexes **1a**/**b** results in the formation of Co(III) η^2-dihydrogen hydride complexes, as shown by analysis of J_{HD} values in partially deuterated species. Rapid exchange between the terminal hydride and the hydrogens of the η^2-dihydrogen results in a single cobalt hydride resonance. These substitutionally labile dihydrogen complexes react with a variety of neutral donor ligands including nitriles, phosphines, and methanol to generate the corresponding $Co(III)(L)(L')H^+$ complexes. Insertion of methyl acrylate into the Co−H bond of **2a**/**b** results in the formation of a mixture of 1,2- and 2,1-insertion products **9a**/**9a′** and **9b**/**9b′**, exhibiting either a four-membered chelate (kinetic product, **9a′**/**9b′**) or five-membered chelate structure. These mixtures ultimately rearrange at 20 °C to form the more stable five-membered chelates **9a** and **9b**. Complex **9a** has been independently synthesized and characterized by single-crystal X-ray diffraction.

Reaction of triethylsilane with these Co(III) alkyl complexes generates two products, the major one of which has been identified as the η^2-silane hydride complex **11a** on the basis of the value of its $^{29}Si-^1H$ coupling constant of 58 Hz. Several other η^2-silane hydride complexes, **11**−**14**, have been generated by addition of silane to the aforementioned η^2-dihydrogen hydride complexes **2a** and **2b**. Only a single hydride resonance for complexes **11**−**13** is seen even at −80 °C, supportive of a rapid dynamic process in which the silyl group slides between hydrides, avoiding a true Co(V) intermediate. Variable-temperature ^1H NMR studies of **14a** containing a prochiral silane, $PhMeSiH_2$, suggest the presence of two distinct pathways for exchange of the terminal Co−H and bridging η^2-SiH. The higher energy process can be frozen out at −78 °C and is proposed to involve silane rotation and formation of a η^2-H_2 ligand, while the lower energy pathway is proposed to involve rapid sliding of the silyl substituent between bridging and terminal hydrides.

These new η^2-H_2 and η^2-silane complexes are suggestive of similar η^2-coordination occurring prior to the cleavage of Co−

Scheme 6. Mechanism Proposed for Hydrogen Scrambling in Diastereomer 14a

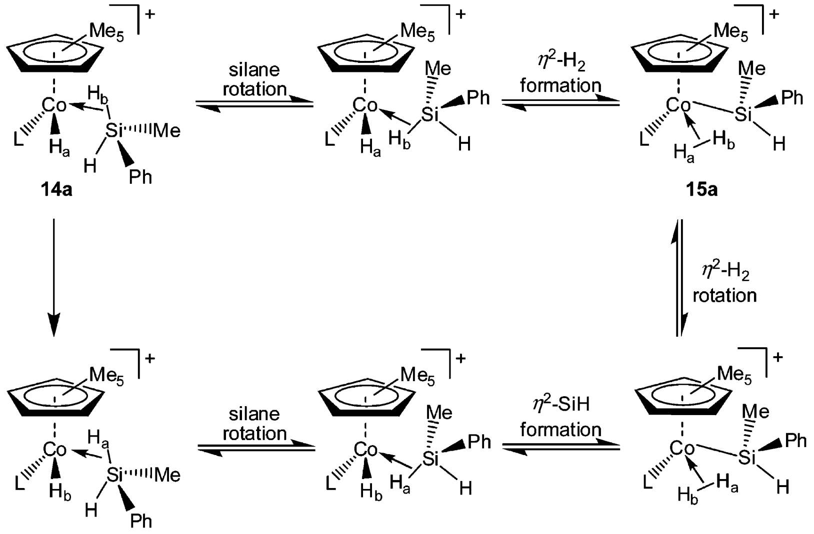

Scheme 7. Proposed Mechanism for Co(III) Alkyl Bond Cleavage in Cp*Co(L)(CH_2CH_2-μ-H)$^+$ Species by H_2 and Silanes, Key Steps in Catalytic Hydrogenation and Hydrosilation (see Scheme 1)

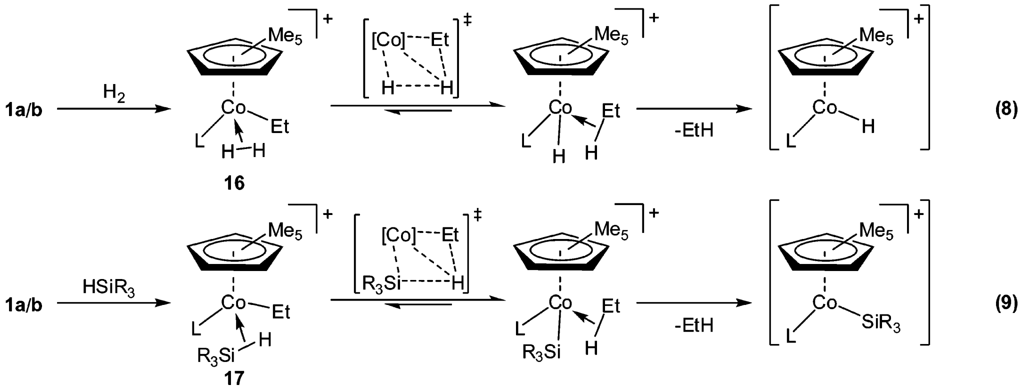

Table 4. Crystallographic Data

	1a·H_2O	**1b**	**9a**
formula	$C_{47}H_{43}F_{24}O_4PBCo$	$C_{47}H_{41}F_{24}PBCo$	$C_{49}H_{43}F_{24}O_5PBCo$
fw	1228.52	1162.51	1268.54
cryst syst	triclinic	orthorhombic	monoclinic
space group	$P\bar{1}$	P*bca*	$P2_1/c$
a (Å)	10.3961(8)	18.1005(4)	12.8214(4)
b (Å)	15.3779(10)	19.3274(4)	21.0585(6)
c (Å)	17.9619(13)	27.7687(6)	19.7828(8)
α (deg)	93.743(5)	90	90
β (deg)	104.803(5)	90	98.726(2)
γ (deg)	105.259(5)	90	90
V (Å^3)	2651.2(3)	9714.5(4)	5279.5(3)
Z	2	8	4
D_{calcd} (Mg/m^3)	1.539	1.590	1.596
λ (Å)	1.54178 (Cu)	0.71073 (Mo)	0.71073 (Mo)
μ (mm^{-1})	3.979	0.513	0.486
cryst dimens (mm^3)	0.20 × 0.15 × 0.15	0.25 × 0.20 × 0.05	0.25 × 0.10 × 0.10
T (K)	100(2)	100(2)	100(2)
θ range (deg)	2.57−65.00	1.47−25.06	1.42−25.00
no. of rflns	28 674	42 497	37 245
no. of indep rflns	8524	8596	9297
R_1	0.0831	0.0420	0.0744
wR_2	0.2127	0.0950	0.1898
R_{all}	0.1111	0.0714	0.1139
GOF	1.050	1.004	1.034

alkyl bonds via a σ-CAM pathway when these agostic alkyl complexes serve as hydrogenation and hydrosilation catalysts.

Experimental Section

General Methods. All manipulations of air- and/or moisture-sensitive compounds were conducted using standard Schlenk techniques. Argon was purified by passage through columns of BASF R3-11 catalyst (Chemalog) and 4 Å molecular sieves. Toluene, pentane, hexane, methylene chloride, and diethyl ether were deoxygenated and dried over a column of activated alumina.[85]

Materials. Acetonitrile, 3,5-bis(trifluoromethyl)benzonitrile, methanol (anhydrous), triethyl amine, 1,2,3,4,5-pentamethylcyclopentadiene (Cp*H), and iodine were used as received from Aldrich. Dicobalt octacarbonyl was purchased from Strem and used as received. Na[B(Ar_F)$_4$][86] (Ar_F = 3,5-$(CF_3)_2C_6H_3$), [H(OEt_2)$_2$]B-(Ar_F)$_4$],[18] **7a**,[19] Cp*Co(P(OMe)$_3$)(C_2H_4).[87,88] and Cp*Co(PMe$_3$)-(C_2H_4)[87,88] were prepared according to literature procedures. Polymer grade ethylene (99.9%) and hydrogen were purchased from National Welders Supply Co. and used as received. Methylene chloride-d_2 was purchased from Cambridge Isotope Laboratories, dried over CaH_2, and degassed using freeze−pump−thaw techniques. Deuterium gas was purchased from Cambridge Isotope Laboratories and used as received. All ^{1}H, ^{13}C, and ^{29}Si{^{1}H} NMR spectra were recorded on Bruker Avance 300, 400, or 500 MHz spectrometers and calibrated at low temperature using MeOH. Chemical shifts are reported relative to internal $CHDCl_2$ (δ 5.32 for ^{1}H) and CD_2Cl_2 (δ 54.00 for ^{13}C) and external $(CH_3)_4Si$ (δ 0.00 for ^{29}Si).

NMR Data for [B(Ar_F)$_4$]$^-$ Anion. The ^{1}H and ^{13}C NMR chemical shifts of the B(Ar_F)$_4^-$ counteranion do not change significantly with temperature and are reported here for all complexes. ^{1}H NMR (CD_2Cl_2): δ 7.70 (8H, s, Ar_F *o*-H), 7.55 (4H, s, Ar_F *p*-H). ^{13}C NMR (CD_2Cl_2): δ 162.0 (q, C_{ipso}, $^1J_{CB}$ = 67 Hz), 135.0 (d, C_{ortho}, $^1J_{CH}$ = 163 Hz), 129.0 (q, C_{meta}, $^2J_{CF}$ = 47 Hz), 125.0 (q, CF_3, $^1J_{CF}$ = 378 Hz), 117.5 (d, C_{para}, $^1J_{CH}$ = 163 Hz).

[Cp*Co(P(OMe)$_3$)(C_2H_4-μ-H)][B(Ar_F)$_4$], 1a. This complex was synthesized according to previously published procedures.[18] X-ray quality crystals of **1a** were obtained by slow vapor diffusion of hexane into a concentrated methylene chloride solution of **1a**.

[Cp*Co(PMe$_3$)(C_2H_4-μ-H)][B(Ar_F)$_4$], 1b. The BF_4^- salt of this complex has been previously reported;[19] however the B(Ar_F)$_4^-$ salt has been isolated here using a procedure analogous to that used to prepare **1a**, and the ^{1}H NMR data for the Cp*Co(PMe$_3$)(C_2H_4-μ-H)$^+$ are consistent with that reported for the BF_4^- complex.[18] A flame-dried Schlenk flask was charged with Cp*Co(PMe$_3$)(C_2H_4) (70 mg, 0.235 mmol) and [H(OEt_2)$_2$][B(Ar_F)$_4$] (214 mg, 0.211 mmol) at room temperature. Methylene chloride (4 mL) was added, and the mixture was stirred until all solids had dissolved (~2−3 min) before cooling to −78 °C for 1−2 h. Hexane (10 mL) was added to precipitate the product, and the reaction mixture was allowed to settle for ~30 min at −78 °C. The red-brown solid was isolated via cannula filtration, washed with hexane (2 × 5 mL), and dried *in vacuo* at room temperature for ~30 min before being stored in the glovebox at −35 °C (219 mg, 89%). X-ray quality crystals were grown by slow evaporation of methylene chloride-d_2

---

[79] Lam, W. H.; Jia, G.; Lin, Z.; Lau, C. P.; Eisenstein, O. *Chem.−Eur. J.* **2003**, *9*, 2775−2782.

[80] Ng, S. M.; Lam, W. H.; Mak, C. C.; Tsang, C. W.; Jia, G.; Lin, Z.; Lau, C. P. *Organometallics* **2003**, *22*, 641−651.

[81] Lachaize, S.; Sabo-Etienne, S.; Donnadieu, B.; Chaudret, B. *Chem. Commun.* **2003**, 214−215.

[82] Hartwig, J. F.; Cook, K. S.; Hapke, M.; Incarvito, C. D.; Fan, Y.; Webster, C. E.; Hall, M. B. *J. Am. Chem. Soc.* **2005**, *127*, 2538−2552.

[83] Webster, C. E.; Fan, Y.; Hall, M. B.; Kunz, D.; Hartwig, J. F. *J. Am. Chem. Soc.* **2003**, *125*, 858−859.

[84] Cleavage of a Ti(IV)−alkyl bond by silanes has been shown to produce a titanium hydride and an alkyl silane, suggesting a very different polarity of the Ti−R bond (relative to the Co−R bonds studied here) with a much higher negative charge on carbon and higher positive charge on the metal, Ti(IV): Koo, K.; Marks, T. J. *J. Am. Chem. Soc.* **1999**, *121*, 8791−8802.

[85] Pangborn, A. B.; Giardello, M. A.; Grubbs, R. H.; Rosen, R. K.; Timmers, F. J. *Organometallics* **1996**, *15*, 1518−1520.

[86] Yakelis, N. A.; Bergman, R. G. *Organometallics* **2005**, *24*, 3579−3581.

[87] Beevor, R. G.; Frith, S. A.; Spencer, J. L. *J. Organomet. Chem.* **1981**, *221*, C25−C27.

[88] Hofmann, L.; Werner, H. *J. Organomet. Chem.* **1985**, *289*, 141−155.

from a concentrated solution of **1b**. ^{1}H NMR (CD_2Cl_2, 500.13 MHz, -82 °C): δ 2.64 (1H, s, $C{-}H_\beta$), 1.58 (15H, s, $C_5(CH_3)_5$), 1.22 (1H, s, $C{-}H_\beta$), 0.993 (9H, d, $P(CH_3)_3$, $^3J_{HP} = 9.5$ Hz), -0.228 (1H, s, $C{-}H_\alpha$), -0.508 (1H, s, $C{-}H_\alpha$), -12.74 (1H, br s, $Co{-}H{-}C$). ^{13}C NMR (CD_2Cl_2, 100.59 MHz, -80 °C): δ 95.0 (s, $\mathit{C}_5(CH_3)_5$), 25.2 (t, C_α, $^1J_{CH} = 159$ Hz), 12.9 (dq, $P(CH_3)_3$, $^1J_{CH} = 129$ Hz, $^2J_{HP} = 30$ Hz), 8.90 (q, $C_5(\mathit{C}H_3)_5$, $^1J_{CH} = 129$ Hz), -5.47 (td, C_β, $^1J_{CH\beta} = 139$ Hz, $^1J_{C-H}{-}Co = 64$ Hz).

$[Cp^*Co(P(OMe)_3)(H)(\eta^2\text{-}H_2)][B(Ar_F)_4]$, 2a. A flame-dried screw cap NMR tube was charged with $[Cp^*Co(P(OMe)_3)(Et)][B(Ar_F)_4]$ (**1a**; 10 mg, 0.0083 mmol) and CD_2Cl_2 (600 μL) and cooled to -78 °C. H_2 ($\sim$20 equiv, 4.0 mL, 0.165 mmol) was added via syringe, and the tube was shaken several times before being placed in a precooled NMR probe at -30 °C. The desired product was generated as the major species in solution (85$-$100% yield) within 30 min at -30 °C and has been characterized *in situ*. ^{1}H NMR (CD_2Cl_2, 500.13 MHz, -30 °C): δ 3.54 (9H, d, $P(OCH_3)_3$, $^3J_{HP} = 11.5$ Hz), 1.87 (15H, s, $C_5(CH_3)_5$), -10.46 (3H, d, $Co(H)(\eta^2\text{-}H_2)$, $^2J_{HP} = 28.5$ Hz). The minor species in solution (0$-$15% yield) has been identified as $[Cp^*Co(P(OMe)_3)(H)(OH_2)][B(Ar_F)_4]$ (**3a**) and has also been characterized *in situ*. ^{1}H NMR (CD_2Cl_2, 500.13 MHz, -30 °C): δ 3.72 (9H, d, $P(OCH_3)_3$), $^3J_{HP} = 11.0$ Hz), 1.61 (15H, s, $C_5(CH_3)_5$), -10.99 (1H, d, $Co{-}H$, $^2J_{HP} = 112.8$ Hz). The resonance of the bound H_2O protons has not been located; this signal is either masked by other resonances or exchange-broadened. Both of these complexes decompose above 0 °C, and attempts to isolate them have been unsuccessful.

$[Cp^*Co(PMe_3)(H)(\eta^2\text{-}H_2)][B(Ar_F)_4]$, 2b. This complex was generated following the previously described procedure for the $[Cp^*Co(P(OCH_3)_3)(H)(\eta^2\text{-}H_2)][B(Ar_F)_4]$ complex starting from $[Cp^*Co(PMe_3)(Et)][B(Ar_F)_4]$ (**1b**, 10 mg, 0.0086 mmol). ^{1}H NMR (CD_2Cl_2, 500.13 MHz, -30 °C): δ 1.87 (15H, s, $C_5(CH_3)_5$), 1.33 (9H, d, $P(CH_3)_3$, $^3J_{HP} = 11.0$ Hz), -10.70 (3H, d, $Co(H)(\eta^2\text{-}H_2)$, $^2J_{HP} = 27.0$ Hz). The minor species in solution (0$-$15% yield) has been identified as $[Cp^*Co(PMe_3)(H)(OH_2)][B(Ar_F)_4]$ (**3b**) and has also been characterized *in situ*. ^{1}H NMR (CD_2Cl_2, 500.13 MHz, -30 °C): δ 1.61 (15H, s, $C_5(CH_3)_5$), 1.41 (9H, d, $P(CH_3)_3$, $^3J_{HP} = 10.5$ Hz), -11.27 (1H, d, $Co{-}H$, $^2J_{HP} = 97.5$ Hz). The chemical shift of the bound H_2O protons has not been located; this signal is either masked by other resonances or exchange-broadened. Both of these complexes decompose above 0 °C, and attempts to isolate them have been unsuccessful.

***In Situ* Generation of $[Cp^*Co(L)(H)(L')][B(Ar_F)_4]$ Complexes from the Corresponding $[Cp^*Co(L)(H)(\eta^2\text{-}H_2)][B(Ar_F)_4]$ Complexes.** The desired ligand, L′, was added via syringe to a screw cap NMR tube at -30 °C containing the appropriate $[Cp^*Co(L)(H)(\eta^2\text{-}H_2)][B(Ar_F)_4]$ complex (generated *in situ* according to the above procedures). The tube was shaken several times before being placed in a precooled NMR probe at -30 °C. The desired products were generated and characterized *in situ* by ^{1}H NMR due to their instability above 0 °C.

$[Cp^*Co(P(OMe)_3)(H)(NCCH_3)][B(Ar_F)_4]$, 4a. This complex was generated quantitatively using the above procedure by adding CH_3CN (1 μL, 0.019 mmol, 2 equiv) to a CD_2Cl_2 solution of **2a**. ^{1}H NMR (CD_2Cl_2, 500.13 MHz, -30 °C): δ 3.61 (9H, d, $P(OCH_3)_3$, $^3J_{HP} = 11.5$ Hz), 2.25 (3H, s, CH_3CN), 1.64 (15H, s, $C_5(CH_3)_5$), -12.54 (1H, d, $Co{-}H$, $^2J_{HP} = 110$ Hz). ^{13}C NMR (CD_2Cl_2, 125.76 MHz, -33 °C): δ 128.5 (s, $CH_3\mathit{C}N$), 97.73 (s, $\mathit{C}_5(CH_3)_5$), 52.91 (d, $P(OCH_3)_3$, $^2J_{CP} = 5.4$ Hz), 9.64 (s, $C_5(\mathit{C}H_3)_5$), 8.71 (s, $\mathit{C}H_3CN$).

$[Cp^*Co(P(OMe)_3)(H)(NCAr_F)][B(Ar_F)_4]$, 5a ($Ar_F = 3,5\text{-}(CF_3)_2\text{-}C_6H_3$). This complex was generated quantitatively using the above procedure by adding 3,5-bis(trifluoromethyl)benzonitrile (1.5 μL, 0.0089 mmol, 1.1 equiv) to a CD_2Cl_2 solution of **2a**. ^{1}H NMR (CD_2Cl_2, 500.13 MHz, -30 °C): δ 8.23 (1H, s, Ar_F *p*-H), 7.98 (2H, s, Ar_F *o*-H), 3.68 (9H, d, $P(OCH_3)_3$, $^3J_{HP} = 11.5$ Hz), 1.71 (15H, s, $C_5(CH_3)_5$), -12.11 (1H, d, $Co{-}H$, $^2J_{HP} = 109$ Hz).

$[Cp^*Co(P(OMe)_3)_2(H)][B(Ar_F)_4]$, 6a. This complex was generated quantitatively using the above procedure by adding $P(OMe)_3$ (1 μL, 0.0083 mmol, 1.0 equiv) to a CD_2Cl_2 solution of **2a**. ^{1}H NMR (CD_2Cl_2, 300.13 MHz, 25 °C): δ 3.62 (18H, virtual t, $P(OCH_3)_3$, $^3J_{apparent} = 12.5$ Hz), 1.78 (15H, s, $C_5(CH_3)_5$), -14.29 (1H, t, $Co{-}H$, $^2J_{HP} = 81$ Hz).

$[Cp^*Co(P(OMe)_3)(H)(MeOH)][B(Ar_F)_4]$, 8a. This complex was generated quantitatively using the above procedure by adding MeOH (1 μL, 0.025 mmol, 3 equiv) to a CD_2Cl_2 solution of **2a**. ^{1}H NMR (CD_2Cl_2, 500.13 MHz, 20 °C): δ 3.94 (1H, br q, $CH_3O\mathit{H}$, $^3J_{HH} = 4.5$ Hz), 3.80 (9H, d, $P(OCH_3)_3$, $^3J_{HP} = 11.0$ Hz), 3.00 (3H, d, $C\mathit{H}_3OH$, $^3J_{HH} = 4.5$ Hz), 1.56 (15H, s, $C_5(CH_3)_5$), -11.52 (1H, d, $Co{-}H$, $^2J_{HP} = 121$ Hz).

$[Cp^*Co(P(OMe)_3)(CH_2CH_2C(O)OCH_3)][B(Ar_F)_4]$, 9a, and $[Cp^*Co(P(OMe)_3)(CH(CH_3)C(O)OCH_3)][B(Ar_F)_4]$, 9a′. These complexes were generated as a 11:1 mixture of **9a′**:**9a** using the above procedure by adding methyl acrylate (1.1 μL, 0.12 mmol, 1.5 equiv) to a CD_2Cl_2 solution of **2a** at -30 °C and monitoring olefin insertion at 0 °C. The ratio of **9a′**:**9a** changed to 1:21 after 24 h at room temperature. **9a**: ^{1}H NMR (CD_2Cl_2, 300.13 MHz, 20 °C) δ 3.78 (9H, d, $P(OCH_3)_3$, $^3J_{HP} = 10.8$ Hz), 3.64 (3H, s, OCH_3), 2.84 (1H, q, CH_2, $^3J_{HH} = 9$ Hz), 2.61 (1H, q, CH_2, $^3J_{HH} = 9$ Hz), 2.4 $-$ 2.2 (2H, overlapping m, CH_2), 1.42 (15H, $C_5(CH_3)_5$). **9a′**: ^{1}H NMR (CD_2Cl_2, 500.13 MHz, 0 °C) δ 3.93 (1H, br s, $C\mathit{H}CH_3$) 3.77 (9H, d, $P(OCH_3)_3$, $^3J_{HP} = 11$ Hz), 3.48 (3H, s, OCH_3), 1.49 (15H, s, $C_5(CH_3)_5$), 1.17 (3H, d, $CHC\mathit{H}_3$, $^3J_{HH} = 7$ Hz).

$[Cp^*Co(P(OMe)_3)(H)(\eta^2\text{-}HSiEt_3)][B(Ar_F)_4]$, 11a. This complex was generated quantitatively using the above procedure by adding Et_3SiH (2 μL, 0.012 mmol, 1.5 equiv) to a CD_2Cl_2 solution of **2a**. ^{1}H NMR (CD_2Cl_2, 400.05 MHz, 25 °C): δ 3.67 (9H, d, $P(OCH_3)_3$, $^3J_{HP} = 12.0$ Hz), 1.86 (15H, s, $C_5(CH_3)_5$), 1.00 (9H, br t, $(C\mathit{H}_3CH_2)_3Si$), 0.55 (6H, br q, $(CH_3C\mathit{H}_2)_3Si$), -13.3 (2H, d, $Co(H)(\eta^2\text{-}SiH)$, $^1J_{HSi(observed)} = 29.0$ Hz, $^2J_{HP} = 51$ Hz). ^{29}Si{^{1}H} DEPT 45 (CD_2Cl_2, 99.36 MHz, -30 °C): δ 20.9 (d, $^2J_{SiP} = 10.9$ Hz).

$[Cp^*Co(P(OMe)_3)(H)(\eta^2\text{-}HSiPh_2H)][B(Ar_F)_4]$, 12a. This complex was generated quantitatively using the above procedure by adding Ph_2SiH_2 (2.5 μL, 0.012 mmol, 1.5 equiv) to a CD_2Cl_2 solution of **2a**. ^{1}H NMR (CD_2Cl_2, 500.13 MHz, -30 °C): δ 7.8$-$7.3 (10H, overlapping m, $(C_6H_5)_2Si$), 5.71 (1H, s, $Si{-}H_{terminal}$, $^1J_{HSi} = 222$ Hz), 3.39 (9H, d, $P(OCH_3)_3$, $^3J_{HP} = 11.5$ Hz), 1.77 (15H, s, $C_5(CH_3)_5$), -12.14 (2H, d, $Co(H)(\eta^2\text{-}HSi)$, $^1J_{HSi(observed)} = 31.5$ Hz, $^2J_{HP} = 46$ Hz). ^{29}Si{^{1}H} DEPT 45 (CD_2Cl_2, 99.35 MHz, -30 °C): δ -2.5 (d, $^2J_{SiP} = 13$ Hz).

$[Cp^*Co(P(OMe)_3)(H)(\eta^2\text{-}HSiPhH_2)][B(Ar_F)_4]$, 13a. This complex was generated quantitatively using the above procedure by adding $PhSiH_3$ (2 μL, 0.017 mmol, 2 equiv) to a CD_2Cl_2 solution of **2a**. ^{1}H NMR (CD_2Cl_2, 400.05 MHz, 25 °C): δ 7.65$-$7.25 (5H, overlapping m, $(C_6H_5)Si$), 4.69 (2H, s, $Si(H_{terminal})_2$, $^1J_{SiH} = 218$ Hz), 3.63 (9H, d, $P(OCH_3)_3$, $^3J_{HP} = 11.6$ Hz), 1.78 (15H, s, $C_5(CH_3)_5$), -12.34 (2H, d, $Co(H)(\eta^2\text{-}SiH)$, $^1J_{HSi(observed)} = 29.0$ Hz, $^2J_{HP} = 44$ Hz). ^{29}Si{^{1}H} DEPT 45 (CD_2Cl_2, 99.35 MHz, -30 °C): δ -28.4 (br s).

$[Cp^*Co(P(OMe)_3)(H)(\eta^2\text{-}HSiPhMeH)][B(Ar_F)_4]$, 14a. This complex was generated quantitatively using the above procedure by adding $PhMeSiH_2$ (2 μL, 0.012 mmol, 1.5 equiv) to a CD_2Cl_2 solution of **2a**. ^{1}H NMR (CD_2Cl_2, 500.13 MHz, -30 °C): δ 7.6$-$7.3 (5H, overlapping m, $(C_6H_5)Si$), 5.04 (1H, s, $Si{-}H_{terminal}$, $^1J_{SiH} = 216$ Hz), 3.64 (9H, d, $P(OCH_3)_3$, $^3J_{HP} = 12$ Hz), 1.69 (15H, s, $C_5(CH_3)_5$), 0.54 (3H, s, $(CH_3)Si$), -12.60 (2H, d, $Co(H)(\eta^2\text{-}SiH)$, $^1J_{SiH(observed)} = 33.5$ Hz, $^2J_{HP} = 45$ Hz). ^{1}H NMR (CD_2Cl_2, 500.13 MHz, -76 °C): δ 7.7$-$7.2 (5H, overlapping m, $(C_6H_5)Si$), 4.97 (1H, s, $Si{-}H_{terminal}$), 3.60 (9H, d, $P(OCH_3)_3$, $^3J_{HP} = 12$ Hz), 1.59 (15H, s, $C_5(CH_3)_5$), 0.40 (3H, s, $(CH_3)Si$), -12.66 (1H, d, $Co(\mathit{H}_A)(\eta^2\text{-}SiH_B)$, $^2J_{HP} = 43.5$ Hz), -12.81 (1H, d, $Co(\mathit{H}_B)(\eta^2\text{-}SiH_A)$, $^2J_{HP} = 43.5$ Hz). ^{29}Si{^{1}H} DEPT 45 (CD_2Cl_2, 99.35 MHz, -30 °C): δ -8.9 (d, $^2J_{SiP} = 12.3$ Hz) Variable-temperature ^{1}H NMR behavior of **14a** is discussed in the text.

[Cp*Co(PMe$_3$)(H)(NCCH$_3$)][B(Ar$_F$)$_4$], 4b. This complex was generated quantitatively using the above procedure by adding CH$_3$CN (1 μL, 0.019 mmol, 2 equiv) to a CD$_2$Cl$_2$ solution of **2b**. ^{1}H NMR (CD$_2$Cl$_2$, 500.13 MHz, −30 °C): δ 2.28 (3H, s, CH$_3$CN), 1.62 (15H, s, C$_5$(CH$_3$)$_5$), 1.36 (9H, d, P(CH$_3$)$_3$, $^2J_{HP}$ = 10 Hz), −13.58 (1H, d, Co−H, $^2J_{HP}$ = 101 Hz).

[Cp*Co(PMe$_3$)(H)(NCAr$_F$)][B(Ar$_F$)$_4$], 5b (Ar$_F$ = 3,5-(CF$_3$)$_2$-C$_6$H$_3$). This complex was generated quantitatively using the above procedure by adding 3,5-bis(trifluoromethyl)benzonitrile (2 μL, 0.012 mmol, 1.4 equiv) to a CD$_2$Cl$_2$ solution of **2b**. ^{1}H NMR (CD$_2$Cl$_2$, 500.13 MHz, −30 °C): δ 8.22 (1H, s, NCAr$_F$ *p*-H), 8.02 (2H, s, NCAr$_F$ *o*-H), 1.69 (15H, s, C$_5$(CH$_3$)$_5$), 1.44 (9H, d, P(CH$_3$)$_3$, $^2J_{HP}$ = 10 Hz), −13.14 (1H, d, Co−H, $^2J_{HP}$ = 98.5 Hz).

[Cp*Co(PMe$_3$)$_2$(H)][B(Ar$_F$)$_4$], 6b. This complex was generated quantitatively using the above procedure by adding PMe$_3$ (1 μL, 0.010 mmol, 1.2 equiv) to a CD$_2$Cl$_2$ solution of **2b**. ^{1}H NMR (CD$_2$Cl$_2$, 500.13 MHz, −30 °C): δ 1.73 (15H, s, C$_5$(CH$_3$)$_5$), 1.39 (18H, br s, P(CH$_3$)$_3$), −16.6 (1H, t, Co−H, $^2J_{HP}$ = 79.5 Hz).

[Cp*Co(PMe$_3$)(H)(P(OMe)$_3$)][B(Ar$_F$)$_4$], 6c. This complex was generated quantitatively using the above procedure by adding P(OMe)$_3$ (1 μL, 0.012 mmol, 1.2 equiv) to a CD$_2$Cl$_2$ solution of **2b**. ^{1}H NMR (CD$_2$Cl$_2$, 500.13 MHz, −30 °C): δ 3.72 (9H, d, P(OCH$_3$)$_3$, $^3J_{HP}$ = 10 Hz), 1.55 (15H, s, C$_5$(CH$_3$)$_5$), 1.32 (9H, br s, P(CH$_3$)$_3$), −15.30 (1H, dd, Co−H, $^2J_{HP}$ = 76 Hz, $^2J_{HP}$ = 85.5 Hz).

[Cp*Co(PMe$_3$)(H)(MeOH)][B(Ar$_F$)$_4$], 8b. This complex was generated quantitatively using the above procedure by adding MeOH (1 μL, 0.025 mmol, 3 equiv) to a CD$_2$Cl$_2$ solution of **2a**. ^{1}H NMR (CD$_2$Cl$_2$, 400.09 MHz, −30 °C): δ 3.94 (1H, br s, CH$_3$O*H*), 2.91 (3H, br s, C*H*$_3$OH), 1.51 (15H, s, C$_5$(CH$_3$)$_5$), 1.34 (9H, br s, P(CH$_3$)$_3$), −11.63 (1H, d, Co−H, $^2J_{HP}$ = 108 Hz).

[Cp*Co(PMe$_3$)(CH$_2$CH$_2$C(O)OCH$_3$)][B(Ar$_F$)$_4$], 9b, and [Cp*Co(PMe$_3$)(CH(CH$_3$)C(O)OCH$_3$)][B(Ar$_F$)$_4$], 9b′. These complexes were generated as a 2:1 mixture of **9b′**:**9b** using the above procedure by adding methyl acrylate (1.2 μL, 0.13 mmol, 1.5 equiv) to a CD$_2$Cl$_2$ solution of **2b** at −30 °C and monitoring olefin insertion at that temperature. Decomposition occurred before complete isomerization could take place. **9b**: ^{1}H NMR (CD$_2$Cl$_2$, 500.13 MHz, −15 °C) δ 3.76 (3H, s, OCH$_3$), 3.04 (1H, q, CH$_2$, J_{HH} = 10 Hz), 2.85 (1H, br t, CH$_2$, J_{HH} = 12 Hz), 2.63 (1H, dd, CH$_2$, J_{HH} = 8.7 Hz, J_{HH} = 19.5 Hz) 2.4 − 2.3 (1H, CH$_2$, hidden under CH$_2$ signal for methyl propionate), 1.50 (15H, d, C$_5$(CH$_3$)$_5$, $^4J_{HP}$ = 1.8 Hz), 1.30 (9H, d, P(CH$_3$)$_3$, $^2J_{HP}$ = 9.8 Hz). **9b′**: ^{1}H NMR (CD$_2$Cl$_2$, 500.13 MHz, −15 °C) δ 3.67 (1H, br s, C*H*CH$_3$), 3.56 (3H, s, OCH$_3$), 1.48 (15H, s, C$_5$(CH$_3$)$_5$), 1.43 (3H, br s, CHC*H*$_3$), 1.37 (9H, d, P(CH$_3$)$_3$, $^2J_{HP}$ = 9.4 Hz).

[Cp*Co(PMe$_3$)(H)(η^2-HSiEt$_3$)][B(Ar$_F$)$_4$], 11b. This complex was generated *in situ* in ~50% conversion using the above procedure by adding Et$_3$SiH (14 μL, 0.086 mmol, 10 equiv) to a CD$_2$Cl$_2$ solution of **2b**. ^{1}H NMR (CD$_2$Cl$_2$, 500.13 MHz, −19 °C): δ 1.80 (15H, s, C$_5$(CH$_3$)$_5$), 1.45 (9H, d, P(CH$_3$)$_3$, $^2J_{HP}$ = 10.5 Hz), −13.96 (2H, d, Co(H)(η^2-SiH), $^1J_{HSi(observed)}$ = 29.0 Hz, $^2J_{HP}$ = 45 Hz). ^{29}Si{^{1}H} DEPT 45 (CD$_2$Cl$_2$, 99.35 MHz, −30 °C): δ 20.7 (br s).

[Cp*Co(PMe$_3$)(H)(η^2-HSiPh$_2$H)][B(Ar$_F$)$_4$], 12b. This complex was generated *in situ* quantitatively using the above procedure by adding Ph$_2$SiH$_2$ (6.4 μL, 0.0344 mmol, 2 equiv) to a CD$_2$Cl$_2$ solution of **2b** (20 mg, 0.0172 mmol of **1b**). ^{1}H NMR (CD$_2$Cl$_2$, 500.09 MHz, −30 °C): δ 7.65 − 7.39 (10H, overlapping m, Ph$_2$Si), 5.80 (1H, s, SiH$_{terminal}$, $^1J_{SiH}$ = 222 Hz), 1.72 (15H, s, C$_5$(CH$_3$)$_5$), 1.14 (9H, d, P(CH$_3$)$_3$, $^2J_{HP}$ = 10.5 Hz), −13.07 (2H, d, Co(H)(η^2-SiH), $^1J_{SiH(observed)}$ = 30 Hz, $^2J_{HP}$ = 44 Hz). ^{29}Si{^{1}H} DEPT 45 (CD$_2$Cl$_2$, 99.35 MHz, −30 °C): δ 0.72 (d, $^2J_{SiP}$ = 14 Hz).

[Cp*Co(PMe$_3$)(H)(η^2-HSiPhH$_2$)][B(Ar$_F$)$_4$], 13b. This complex was generated *in situ* quantitatively using the above procedure by adding PhSiH$_3$ (4.3 μL, 0.0344 mmol, 2 equiv) to a CD$_2$Cl$_2$ solution of **2b** (20 mg, 0.0172 mmol of **1b**). ^{1}H NMR (CD$_2$Cl$_2$, 500.09 MHz, −30 °C): δ 7.80−7.30 (5H, overlapping m, PhSi), 4.69 (2H, s, Si(H$_{terminal}$)$_2$, $^1J_{SiH}$ = 218 Hz), 1.69 (15H, s, C$_5$(CH$_3$)$_5$), 1.51 (9H, d, P(CH$_3$)$_3$, $^2J_{HP}$ = 7.5 Hz), −13.14 (2H, d, Co(H)(η^2-SiH), $^1J_{SiH(observed)}$ = 29 Hz, $^2J_{HP}$ = 43.5 Hz). ^{29}Si{^{1}H} DEPT 45 (CD$_2$Cl$_2$, 99.35 MHz, −30 °C): δ −26.7 (d, $^2J_{SiP}$ = 14 Hz).

[Cp*Co(PMe$_3$)(H)(η^2-HSiPhMeH)][B(Ar$_F$)$_4$], 14b. This complex was generated *in situ* quantitatively using the above procedure by adding PhMeSiH$_2$ (4.7 μL, 0.0344 mmol, 2 equiv) to a CD$_2$Cl$_2$ solution of **2b** (20 mg, 0.0172 mmol of **1b**). ^{1}H NMR (CD$_2$Cl$_2$, 500.09 MHz, −30 °C): δ 7.70−7.30 (5H, overlaping m, PhSi), 5.03 (1H, s, SiH$_{terminal}$, $^1J_{SiH}$ = 219 Hz), 1.71 (15H, s, C$_5$(CH$_3$)$_5$), 1.40 (9H, d, P(CH$_3$)$_3$, $^2J_{HP}$ = 10.5 Hz), 0.81 (3H, br s, CH$_3$Si), −13.15 (2H, d, Co(H)(η^2SiH), $^1J_{SiH(observed)}$ = 28.5 Hz, $^2J_{HP}$ = 44.5 Hz). ^{29}Si{^{1}H} DEPT 45 (CD$_2$Cl$_2$, 99.35 MHz, −30 °C): δ −9.0 (d, $^2J_{SiP}$ = 13.5 Hz).

Deprotonation of [Cp*Co(L)(η^2-H$_2$)(H)][B(Ar$_F$)$_4$], 2a and 2b. A solution of **2a** or **2b** was generated in an NMR tube as described previously in CD$_2$Cl$_2$. NEt$_3$ (1 − 1.5 equiv) was added to these solutions at 20 °C via syringe, and the tubes were briefly shaken to ensure complete mixing. Cp*Co(L)(H)$_2$ complexes **10a** and **10b** were generated quantitatively and characterized *in situ*. Cp*Co(P(OMe)$_3$)(H)$_2$, **10a**: ^{1}H NMR (CD$_2$Cl$_2$, 500.13 MHz, −30 °C) δ 3.41 (9H, d, P(OCH$_3$)$_3$, $^3J_{HP}$ = 11.5 Hz), 1.85 (15H, s, C$_5$(CH$_3$)$_5$), −17.23 (2H, d, Co(H)$_2$, $^2J_{HP}$ = 97.5 Hz). Cp*Co(PMe$_3$)(H)$_2$, **10b**: ^{1}H NMR (CD$_2$Cl$_2$, 500.13 MHz, −30 °C), δ 1.84 (15H, s, C$_5$(CH$_3$)$_5$), 1.17 (9H, d, P(CH$_3$)$_3$, $^2J_{HP}$ = 9.5 Hz), −18.09 (2H, d, Co(H)$_2$, $^2J_{HP}$ = 88.5 Hz).

General Procedure for Generating Partially Deuterated [Cp*(L)Co(H)(η^2-H$_2$)][B(Ar$_F$)$_4$] Complexes, 2a-d_n and 2b-d_n. A solution of the corresponding [Cp*Co(L)(H)(η^2-H$_2$)][B(Ar$_F$)$_4$] complex in methylene chloride-d_2 was degassed via two freeze−pump−thaw cycles, back-filled with D$_2$ gas, and stored at −78 °C. The tube was then briefly shaken before being placed in a precooled NMR probe at −71 °C, at which point the reaction was monitored by ^{1}H NMR.

[Cp*Co(P(OMe)$_3$)(CH$_2$CH$_2$C(O)OCH$_3$)][B(Ar$_F$)$_4$], 9a. A flame-dried Schlenk flask was charged with **1a** (200 mg, 0.165 mmol), methyl acrylate (297 μL, 3.30 mmol, 20 equiv), and methylene chloride (5 mL) under an atmosphere of Ar at room temperature. The solution was allowed to stir for 5−10 min before purging with H$_2$ for 15 min, at which point the solution was sealed off from Ar and H$_2$ and allowed to stir at room temperature for 2 h. The solution was then concentrated under vacuum to ~ 1−2 mL, and hexane (8 mL) was added. Volatiles were removed *in vacuo* with stirring to give a brown powder (178 mg, 0.140 mmol, 85%), which was then dried under vacuum for an additional 1 h before being stored in a glovebox at −35 °C. X-ray quality crystals were grown by vapor diffusion of pentane into a concentrated 50:50 mixture of toluene and methylene chloride solution of **9a**. ^{1}H NMR data are identical to those obtained upon *in situ* formation of **9a** from **2a**. ^{13}C{^{1}H} NMR (CD$_2$Cl$_2$, 125.77 MHz, 20 °C): δ 191.5 (s, C=O), 96.6 (s, *C*$_5$(CH$_3$)$_5$), 55.7 (s, OCH$_3$), 54.9 (d, P(OCH$_3$)$_3$, $^2J_{CP}$ = 8 Hz), 38.5 (s, β-CH$_2$), 9.2 (s, C$_5$(*C*H$_3$)$_5$), 7.3 (s, α-CH$_2$). Anal. Calcd for C$_{49}$H$_{43}$F$_{24}$O$_5$BPCo: C, 46.39; H, 3.42. Found: C, 46.15; H, 3.17.

Isomerization of 9a′ to 9a in the Absence of H$_2$. A ~8:1 mixture of **9a′**:**9a** was generated from **2a** and methyl acrylate in a J-Young NMR tube as described above. Upon consumption of **2a**, excess H$_2$ was removed from the reaction via three freeze−pump−thaw cycles. The reaction was then monitored via ^{1}H NMR over the course of 24 h at 20 °C resulting in a 1:11 ratio of **9a′**:**9a**.

Acknowledgment. We thank the National Science Foundation (CHE-0615704) for support of this work.

Supporting Information Available: CIF files giving complete crystallographic data for complexes **1a**·H$_2$O, **1b**, and **9a**. This material is available free of charge via the Internet at http://pubs.acs.org.

OM700620W